Electronic Supporting Information

Room temperature red phosphorescence: enhancing and regulating phosphorescence by exploiting intermolecular halogen interactions and thermal stimuli

Tsutomu Ishi-i,[*a] Yuugo Shibata,[a,b] , Rintaro Homei,[a] Taisuke Matsumoto,[c] Jun Hyeon Lee,[d] and Takuma Yasuda[*d,e]

Table of Contents

Experimental Section

General. All melting points are uncorrected. ATR-IR spectra were recorded on a JASCO FT/IR-470 plus Fourier transform infrared spectrometer, equipped with ATR PRO attachment (Zn-Se prism). ^{1}H and ^{13}C NMR spectra were determined in $CDCl_3$ with a JEOL ECX 500 spectrometer. Residual solvent protons were used as internal standard and chemical shifts (δ) are given relative to tetramethylsilane (TMS). The coupling constants (J) are reported in hertz (Hz). Elemental analysis was performed at the Elemental Analytical Center, Kyushu University. Fast atom bombardment mass spectrometry (FAB-MS) spectra were recorded with a JEOL JMS-70 mass spectrometer with m-nitrobenzyl alcohol (NBA) as a matrix. Gel permeation chromatography (GPC) was performed with a Japan Analytical Industry LC-908 using JAIGEL-1H column (20 × 600 mm) and JAIGEL-2H column (20 × 600 mm) eluting with chloroform (3.0 mL/min). Analytical TLC was carried out on silica gel coated on aluminum foil (Merck 60 F254). Column chromatography was carried out on silica gel (WAKO C300). 4,7-Dibromo-5,6-dimethoxy-2,1,3-benzothiadiazole (BTD(OMe)-Br)[1] was prepared according to the methods reported previously.

1 T. Ishi-i, R. Kichise, I. S. Park, T. Yasuda and T. Matsumoto, *J. Mater. Chem. C*, 2023, **11**, 3003–3009.

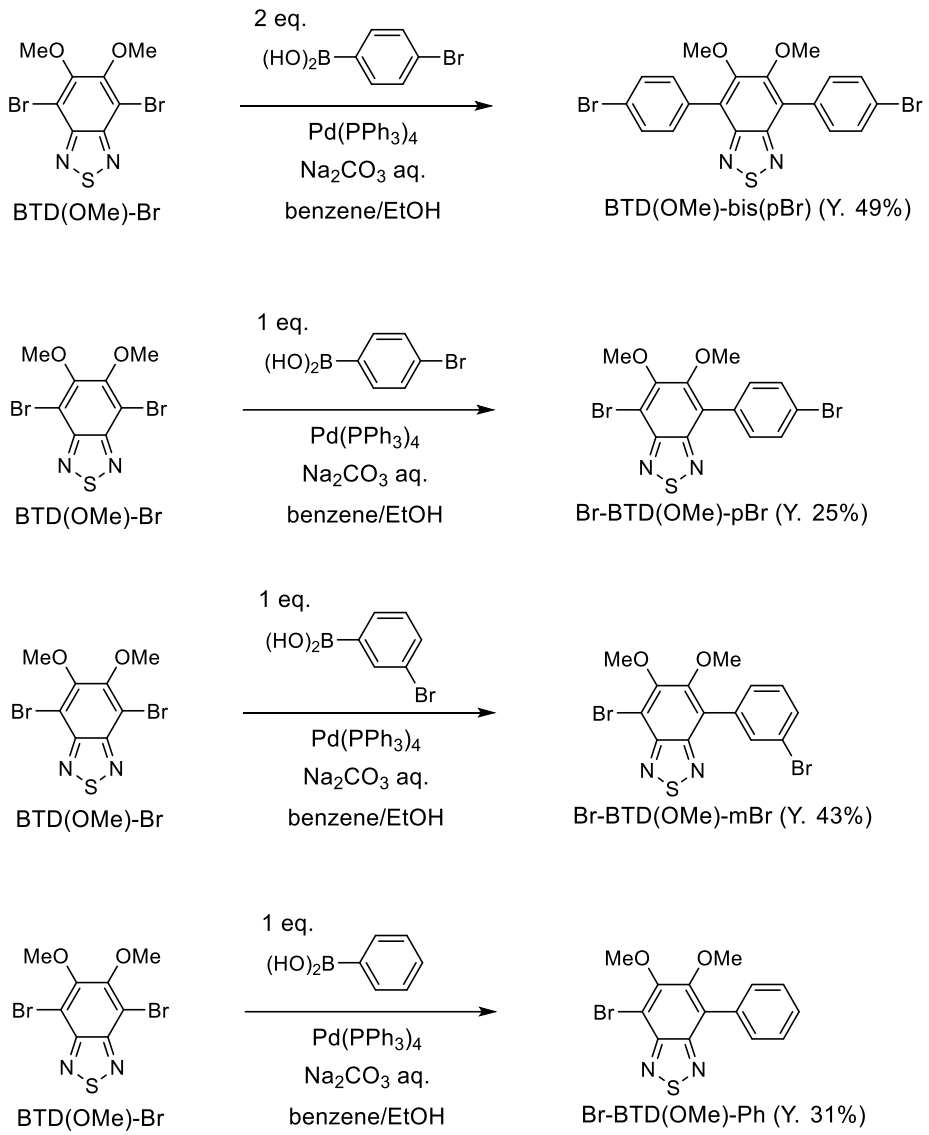

Scheme S1 Preparation of benzothiadiazole-based dyes.

4,7-Bis(4-bromophenyl)-5,6-dimehoxy-2,1,3-benzothiadiazole (BTD(OMe)-bis(pBr)). To a mixture of BTD(OMe)-Br (177 mg, 0.5 mmol), 4-bromophenylbronic acid (221 mg, 1.1 mmol), and tetrakis(triphenylphosphine)palladium(0) (58 mg, 0.05 mmol) were added in deaerated benzene (10 mL), ethanol (2.5 mL), and 2 M aqueous solution of sodium carbonate (5 mL). Then the mixture was heated at 85 °C for 18 h under an argon atmosphere. After the reaction mixture was poured into water, it was extracted with dichloromethane. The combined organic layer was washed with brine and water, dried over anhydrous magnesium sulfate, and evaporated in vacuo to dryness. The residue was purified by silica gel column chromatography (WAKO C300) eluting with chloroform/hexane (1:2, v/v) and by GPC eluting with

chloroform to give BTD(OMe)-bis(pBr) in 49% (124 mg, 0.245 mmol). An analytical sample was obtained by recrystallization from dichloromethane/hexane to give pale yellow needles: mp 209–210 °C; IR (ATR, Zn-Se) 3071, 2931, 2843, 1455, 1369, 1293, 1277, 1050, 1009, 985, 956, 892, 878, 825, 811, 764, 666; ^{1}H NMR ($CDCl_3$, 500 MHz) δ 3.79 (s, 6 H, OMe), 7.62 (d, J = 8.6 Hz, 4 H, ArH), 7.68 (d, J = 8.6 Hz, 4 H, ArH); ^{13}C NMR ($CDCl_3$, 126 MHz) δ 61.58 (OMe), 122.56, 123.50, 131.46, 132.14, 132.18, 151.68, 153.42; FAB-MS (positive, NBA) m/z 505, 507, 509 [$(M+1)^+$]. Anal. Calcd for $C_{20}H_{14}Br_2N_2O_2S$ (506.21): C, 47.45; H, 2.79; N, 5.53. Found: C, 47.32; H 2.68; N, 5.69.

4-Bromo-7-(4-bromophenyl)-5,6-dimehoxy-2,1,3-benzothiadiazole (Br-BTD(OMe)-pBr). To a mixture of BTD(OMe)-Br (531 mg, 1.5 mmol), 4-bromophenylbronic acid (301 mg, 1.5 mmol), and tetrakis(triphenylphosphine)palladium(0) (87 mg, 0.075 mmol) were added in deaerated benzene (30 mL), ethanol (7.5 mL), and 2 M aqueous solution of sodium carbonate (15 mL). Then the mixture was heated at 85 °C for 5 h under an argon atmosphere. After the reaction mixture was poured into water, it was extracted with dichloromethane. The combined organic layer was washed with brine and water, dried over anhydrous magnesium sulfate, and evaporated in vacuo to dryness. The residue was purified by silica gel column chromatography (WAKO C300) eluting with chloroform/hexane (3:7, v/v) and by GPC eluting with chloroform to give Br-BTD(OMe)-pBr in 25% (163 mg, 0.379 mmol). An analytical sample was obtained by recrystallization from dichloromethane/hexane to give pale yellow prisms: mp 154–155 °C; IR (ATR, Zn-Se) 3011, 2974, 2937, 2837, 1454, 1407, 1383, 1295, 1281, 1047, 1010, 981, 886, 832, 819, 792, 742; ^{1}H NMR ($CDCl_3$, 126 MHz) δ 3.74 (s, 3 H, OMe), 4.07 (s, 3 H, OMe), 7.55 (d, J = 8.0 Hz, 2 H, ArH), 7.65 (d, J = 8.0 Hz, 2 H, ArH); ^{13}C NMR ($CDCl_3$, 126 MHz) δ 61.43, 61.74 (OMe), 105.84, 122.77, 123.50, 131.51, 131.59, 132.04, 150.93, 151.14, 153.49, 154.81; FAB-MS (positive, NBA) m/z 429, 431, 433 [$(M+1)^+$]. Anal. Calcd for $C_{14}H_{10}Br_2N_2O_2S$ (430.11): C, 39.10; H, 2.34; N, 6.51. Found: C, 39.22; H, 2.28; N, 6.56.

4-Bromo-7-(3-bromophenyl)-5,6-dimehoxy-2,1,3-benzothiadiazole (Br-BTD(OMe)-mBr). To a mixture of BTD(OMe)-Br (531 mg, 1.5 mmol), 3-bromophenylbronic acid (301 mg, 1.5 mmol), and

tetrakis(triphenylphosphine)palladium(0) (87 mg, 0.075 mmol) were added in deaerated benzene (30 mL), ethanol (7.5 mL), and 2 M aqueous solution of sodium carbonate (15 mL). Then the mixture was heated at 85 °C for 7 h under an argon atmosphere. After the reaction mixture was poured into water, it was extracted with dichloromethane. The combined organic layer was washed with brine and water, dried over anhydrous magnesium sulfate, and evaporated in vacuo to dryness. The residue was purified by silica gel column chromatography (WAKO C300) eluting with chloroform/hexane (3:7, v/v) and by GPC eluting with chloroform to give Br-BTD(OMe)-mBr in 43% (280 mg, 0.651 mmol). An analytical sample was obtained by recrystallization from dichloromethane/hexane to give pale yellow needles: mp 95–96 °C; ATR-IR (Zn-Se, cm^{-1}) 3064, 2994, 2937, 2834, 1457, 1385, 1276, 1049, 957, 882, 800, 783, 715, 681; ^{1}H NMR ($CDCl_3$, 500 MHz) δ 3.77 (s, 3 H, OMe), 4.08 (s, 3 H, OMe), 7.40 (t, J = 7.8 Hz, 1 H, ArH), 7.58–7.62 (m, 2 H, ArH), 7.82 (s, 1 H, ArH); ^{13}C NMR ($CDCl_3$, 126 MHz) δ 61.43, 61.83 (OMe), 106.08, 122.24, 123.16, 129.05, 129.75, 131.44, 133.27, 134.69, 150.89, 151.08, 153.66, 154.75; FAB-MS (positive, NBA) m/z 429, 431, 433 [$(M+1)^+$]. Anal. Calcd for $C_{14}H_{10}Br_2N_2O_2S$ (430.11): C, 39.10; H, 2.34; N, 6.51. Found: C, 39.17; H 2.39; N, 6.44.

4-Bromo-5,6-dimehoxy-7-phenyl-2,1,3-benzothiadiazole (Br-BTD(OMe)-Ph). To a mixture of BTD(OMe)-Br (177 mg, 0.5 mmol), phenylboronic acid (61 mg, 0.5 mmol), and tetrakis(triphenylphosphine)palladium(0) (29 mg, 0.025 mmol) were added in deaerated benzene (10 mL), ethanol (2.5 mL), and 2 M aqueous solution of sodium carbonate (5 mL). Then the mixture was heated at 85 °C for 7 h under an argon atmosphere. After the reaction mixture was poured into water, it was extracted with dichloromethane. The combined organic layer was washed with brine and water, dried over anhydrous magnesium sulfate, and evaporated in vacuo to dryness. The residue was purified by silica gel column chromatography (WAKO C300) eluting with dichloromethane/hexane (1:2, v/v) and by GPC eluting with chloroform to give Br-BTD(OMe)-Ph in 31% (55 mg, 0.157 mmol). An analytical sample was obtained by recrystallization from dichloromethane/hexane to give pale yellow prisms: mp 105–106 °C; ATR-IR (Zn-Se, cm^{-1}) 3063, 3018, 2996, 2938, 2849, 1456, 1389, 1281, 1206, 1132, 1039, 973, 882, 830, 769, 727, 710, 695, 637; ^{1}H NMR ($CDCl_3$, 500 MHz) δ 3.75 (s, 3 H, OMe), 4.09 (s, 3 H, OMe), 7.48 (t, J = 7.6 Hz, 1 H, ArH),

7.53 (t, J = 7.6 Hz, 2 H, ArH), 7.65 (d, J = 7.6 Hz, 2 H ArH); ^{13}C NMR ($CDCl_3$, 126 MHz) δ 61.41, 61.71 (OMe), 105.33, 124.74, 128.30, 128.46, 130.28, 132.76, 151.10, 151.38, 153.47, 154.84; FAB-MS (positive, NBA) m/z 351, 353 [$(M+1)^+$]. Anal. Calcd for $C_{14}H_{11}BrN_2O_2S$ (351.22): C, 47.88; H, 3.16; N, 7.98. Found: C, 47.96; H 3.05; N, 8.00.

Instrumentation. Steady-state photoluminescence spectra and excitation spectra were measured on a JASCO FP-8600 fluorescence spectrophotometer. Absorption spectra were measured on a JASCO V-570 spectrophotometer. Diffuse reflection spectra were measured on a JASCO V-670 spectrophotometer equipped with a JASCO ISV-922 integrating sphere system. The fluorescence and phosphorescence quantum yields were measured with an absolute photoluminescence quantum yield measurement system (Hamamatsu Photonics, Quantaurus-QY C11347-01 and C9920-01). This instrument consisted of an integrating sphere equipped with a monochromatized Xe arc lamp as the light source and a multichannel spectrometer. The sensitivity of this system was fully calibrated using deuterium and halogen standard light sources. Fluorescence lifetime measurements were made by using a laser diode (340 nm, pulse width 100 ps, repetition rate 20 kHz) and as the excitation light source and a time-correlated single-photon counting fluorometer (Hamamatsu Photonics, Quantaurus-Tau C11367). For phosphorescence lifetime measurements, a LED diode (340 nm, pulse width 1 ns, repetition rate 2 kHz) was used as the excitation light source. The analysis of the fluorescence and phosphorescence decay curves were carried out using the deconvolution method. Differential scanning calorimetry was performed on a METTLER TOLEDO DSC822e at heating and cooling rates of 10 K min^{-1} under a nitrogen atmosphere. Powder X-ray diffraction measurements were performed on RIGAKU RINT-TTR III and carried out with Cu(Kα) radiation from an X-ray tube with a 0.5 × 10 mm^2 filament operated at 50 kV × 300 mA (15 kW).

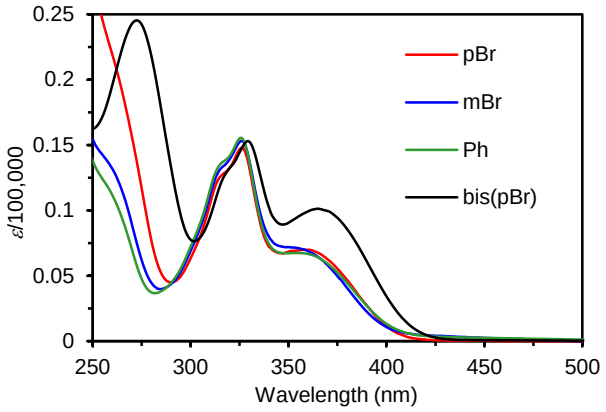

Fig. S1 UV/Vis absorption spectra of Br-BTD(OMe)-pBr, Br-BTD(OMe)-mBr, Br-BTD(OMe)-Ph, and BTD(OMe)-bis(pBr) in THF (1.0×10^{-5} M).

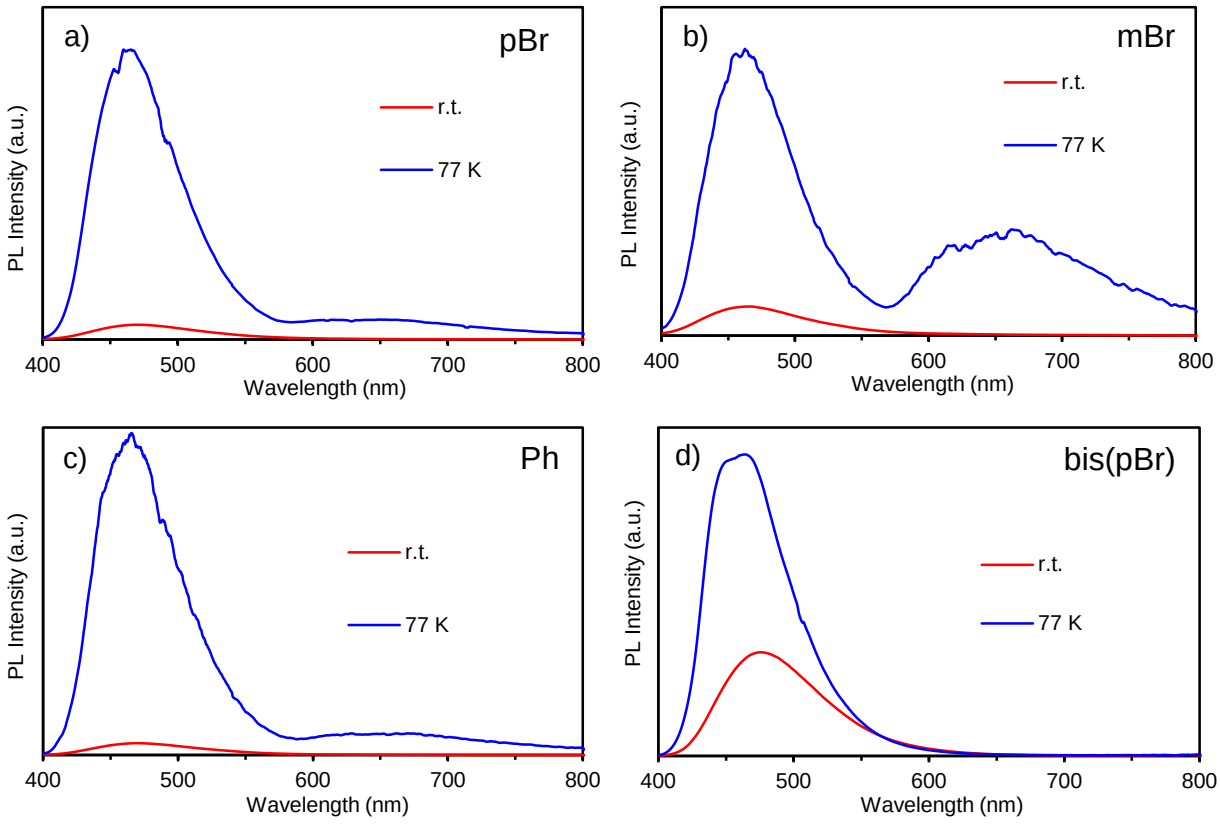

Fig. S2 Steady-state photoluminescence spectra (excited at 350 nm) of (a) Br-BTD(OMe)-pBr, (b) Br-BTD(OMe)-mBr, (c) Br-BTD(OMe)-Ph, and (d) BTD(OMe)-bis(pBr) in THF (1×10^{-5} M) at room temperature and 77 K under air atmosphere.

Table S1. Spectral data of benzothiadiazole-based dyes in THF,[a]

Comp.	Temp.	λ_{abs} (nm)	ε	ex (nm)	λ_{em} (nm)	Φ_F (%) [b]	Φ_P (%) [b]
Br-BTD(OMe)-pBr	r.t.	370 (sh) [c]	6,700	350	469	0.5	
		326	14,790				
		315 (sh) [c]	12,570				
	77 K			350	ca. 650	13.6	1.5
					464		
Br-BTD(OMe)-mBr	r.t.	365 (sh) [c]	6,450	350	462	0.2	
		326	15,330				
		315 (sh) [c]	13,140				
	77 K			350	662	1.2	0.9
					462		
Br-BTD(OMe)-Ph	r.t.	365 (sh) [c]	6,420	350	470	0.7	
		326	15,550				
		315 (sh) [c]	13,510				
	77 K			350	661	17.5	2.7
					464		
BTD(OMe)-bis(pBr)	r.t.	365	10,130	350	476	14.7	
		329	15,300				
		315 (sh) [c]	11,900				
		272	24,530				
	77 K			350	464	36.2	
					450 (sh) [c]		

[a] 1×10^{-5} M, [b] determined relative to quinine sulfate (Φ_{FL} 0.55, ex 350 nm) in sulfuric acid, [c] sh is the abbreraviation of shoulder.

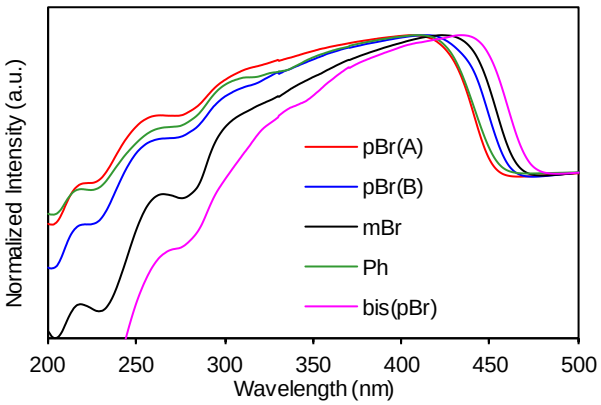

Fig. S3 Diffuse reflection UV/Vis spectra of Br-BTD(OMe)-pBr(A), Br-BTD(OMe)-pBr(B), Br-BTD(OMe)-mBr, Br-BTD(OMe)-Ph, and BTD(OMe)-bis(pBr) in the crystalline solid state.

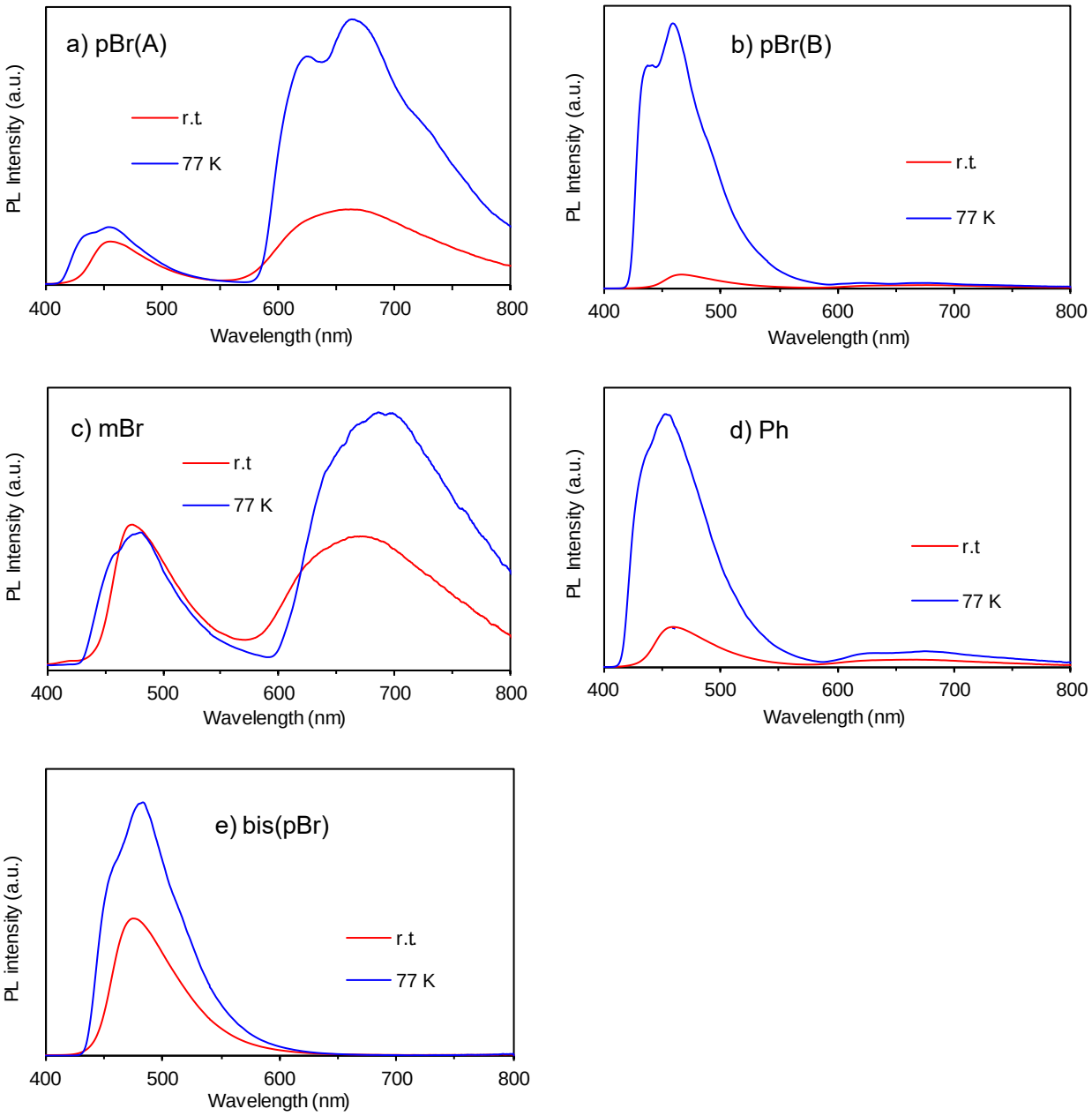

Fig. S4 Steady-state photoluminescence spectra (excited at 300 nm) of (a) Br-BTD(OMe)-pBr(A), (b) Br-BTD(OMe)-pBr(B), (c) Br-BTD(OMe)-mBr, (d) Br-BTD(OMe)-Ph, and (e) Br-BTD(OMe)-bis(pBr) (excited at 350 nm) in the crystalline solid state at room temperature and 77 K under air atmosphere.

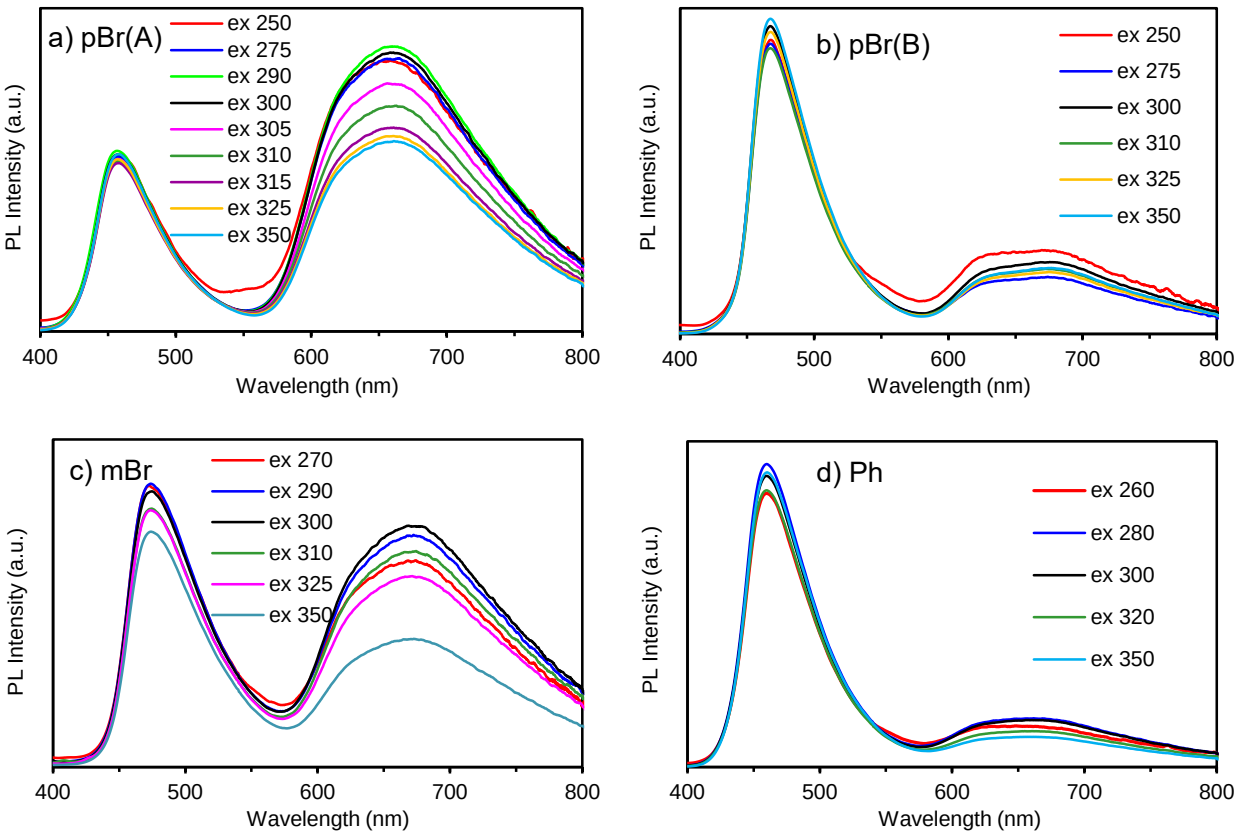

Fig. S5 Excitation dependence of steady-state photoluminescence spectra (excited at 250–350 nm) of (a) Br-BTD(OMe)-pBr(A), (b) Br-BTD(OMe)-pBr(B), (c) Br-BTD(OMe)-mBr, and (d) Br-BTD(OMe)-Ph in the crystalline solid state.

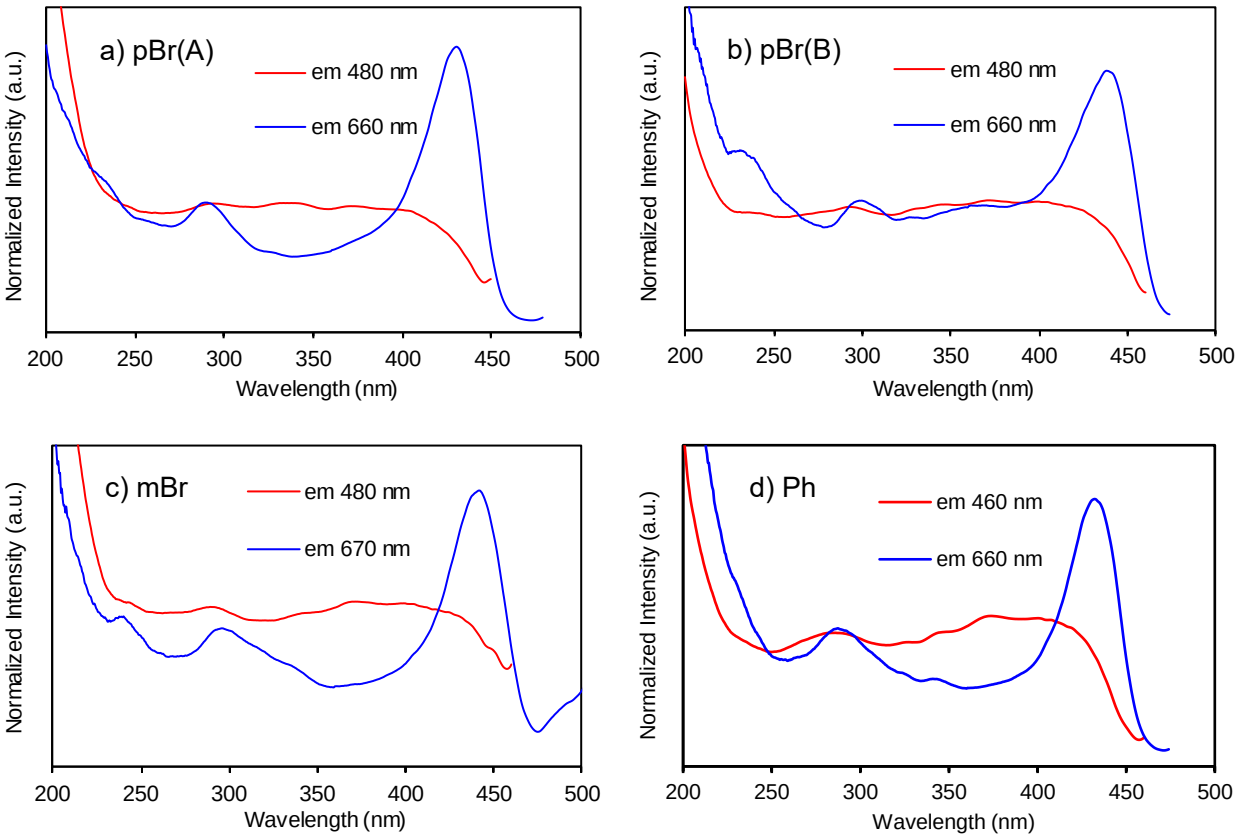

Fig. S6 Excitation spectra of (a) Br-BTD(OMe)-pBr(A), (b) Br-BTD(OMe)-pBr(B), (c) Br-BTD(OMe)-mBr, and (d) Br-BTD(OMe)-Ph in the crystalline solid state.

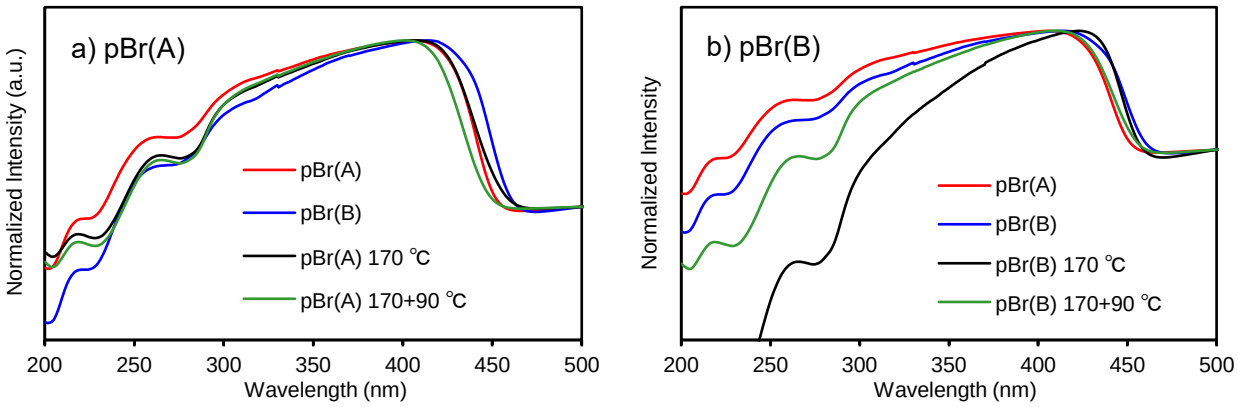

Fig. S7 Diffuse reflection spectra of (a) Br-BTD(OMe)-pBr(A) and (b) Br-BTD(OMe)-pBr(B) before and after heating at 90 °C and 90+170 °C.

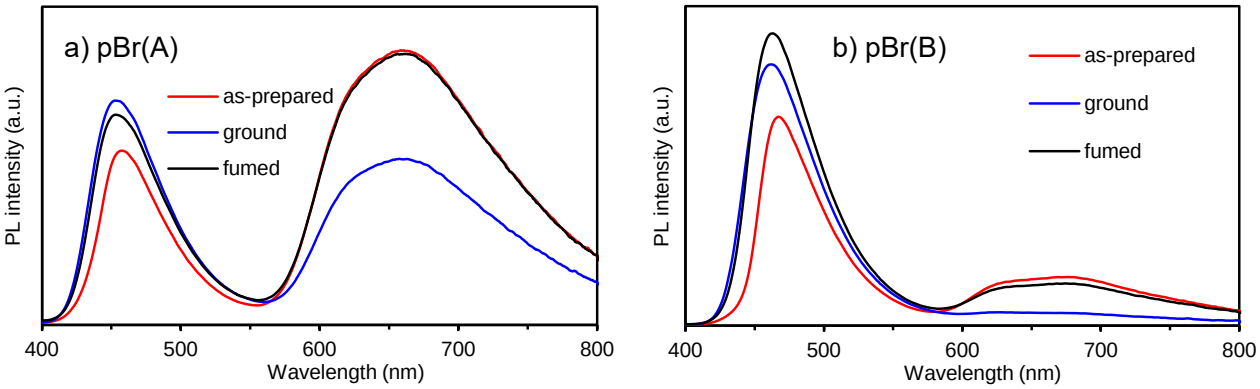

Fig. S8 Steady-state photoluminescence spectra (excited at 300 nm) of the as-prepared, ground, and fumed (dichloromethane-vapor) samples for (a) Br-BTD(OMe)-pBr(A) and (b) Br-BTD(OMe)-pBr(B).

Table S2 Spectral data of benzothiadiazole-based dyes in the crystalline solid state,

Comp.	λ_{abs} (nm)	Fluorescence [a]				Phosphorescence [a]			
		λ_F (nm)	Φ_F (%) [b]	em (nm)	λ_{ex} (nm)	λ_P (nm)	Φ_P (%) [b,c]	em (nm)	λ_{ex} (nm)
Br-BTD(OMe)-pBr(A)	405 316 (sh)[d] 264 220	458	0.6	480	415 (sh) [d] 371 333 294	660	6.2	660	431 290
77 K	–	454	1.0	480	413(sh) [d] 376 342 330 290 261	662 623	20.2	660	406 286
ground	392 260 220	453	–	480	415(sh) [d] 375 348 290	660	–	660	419 290
fumed	404 260 220	454	–	480	415(sh) [d] 397 373 292	660	–	660	425 290
170 °C	406 330 266 219	466	1.0	–	–	– [e]	~0 [e]	–	–
170 + 90 °C	402 330 266 218	456	0.6	–	–	660	5.9	–	–
Br-BTD(OMe)-pBr(B)	415 305 (sh) [d] 265 218	467	1.0	480	404 372 345 292 236	678 625 (sh) [d]	2.4	670	439 361 330 299 233 (sh) [d]
77 K	–	456 437	23.8	480	413(sh) [d] 405 343 298	673 622	4.3	670	422 346 327 297 229
ground	407 331 265 220	462	–	480	425(sh) [d] 400 373 347	628	–	670	431 347 296

					293				
					277				
					261				
					236				
fumed	407	463	–	480	404	675	–	670	436
	305 (sh) [d]				373	625 (sh) [d]			347
	260				348				327
	217				292				297
					238				231
170 °C	–	466	1.0	–	–	– [e]	~0 [e]	–	–
170 + 90 °C	–	456	0.6	–	–	660	5.6	–	–
Br-BTD(OMe)-mBr	423	474	0.7	480	399	672	3.2	670	443
	305 (sh) [d]				372				297
	265				345 (sh) [d]				241
	218				290				
					243				
77 K	–	481	0.8	480	399	692	6.1	670	426
					368				337
					343				294
					285				238
Br-BTD(OMe)-Ph	411	460	1.2	460	410 (sh) [d]	662	1.7	660	432
	305 (sh) [d]				373				341
	260 (sh) [d]				345 (sh) [d]				288
	219				328				
					286				
77 K	–	453	9.4	460	381	674	3.4	660	413
					374				341
					352				324
					343				282
					335				231
					297				
					264				
BTD(OMe)-bis(pBr)	434	478	27.6	490	440 (sh) [d]	– [f]	0	–	–
	340 (sh) [d]				405				
					398				
					372				
					297				
					261				
					257				
77 K	–	483	58.3	–	–	– [f]	0	–	–
		455(sh) [d]							

[a] excited at 300 nm, [b] absolute fluorescence and phosphorescence quantum yields determined by an integrating sphere system, [c] the contribution of fluorescence can be regarded as negligible, because of the absence of short-lived component, [d] sh is the abbreraviation of shoulder, [e] observed as tail, [f] not oberved.

Table S3 Fluorescence and phosphorescence quantum yields of benzothiadiazole-based dyes in the crystalline solid state,

Comp.	Conditions	Ex. (nm)	Φ_F (%) [a]	Φ_P (%) [a,b]
Br-BTD(OMe)-pBr(A)	r.t.	350	0.6	4.2
		325	0.6	4.3
		310	0.6	5.0
		300	0.6	6.2
		290	0.6	6.3
		275	0.6	6.1
		250	0.6	6.0
	77 K	300	1.0	20.2
		275	1.0	19.7
	170 °C	350	1.0	~0
		300	1.0	~0
	170 + 90 °C	350	0.6	3.5
		300	0.6	5.9
Br-BTD(OMe)-pBr(B)	r.t.	350	1.0	2.2
		325	1.0	2.2
		300	1.0	2.4
		275	0.9	2.0
		250	0.9	1.8
	77 K	300	23.8	4.3
		275	21.7	3.5
	170 °C	300	1.0	~0
	170 + 90 °C	300	0.6	5.6
Br-BTD(OMe)-mBr	r.t.	350	0.6	1.7
		325	0.7	2.5
		310	0.7	2.8
		300	0.7	3.2
		290	0.7	3.0
		270	0.7	2.7
	77 K	300	0.8	6.1
Br-BTD(OMe)-Ph	r.t.	350	1.2	1.2
		320	1.2	1.4
		300	1.2	1.7
		280	1.1	1.9
		260	1.1	1.7
	77 K	300	9.4	3.4
BTD(OMe)-bis(pBr)	r.t.	350	27.6	–
	77 K	350	58.3	–

[a] absolute fluorescence and phosphorescence quantum yields determined by an integrating sphere system, [b] the contribution of fluorescence can be regarded as negligible, because of the absence of short-lived component.

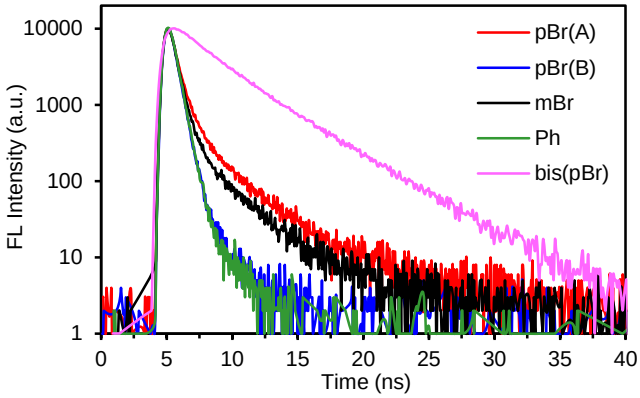

Fig. S9 Fluorescence decay curves (monitored at 460 nm) of Br-BTD(OMe)-pBr(A), Br-BTD(OMe)-pBr(B), Br-BTD(OMe)-mBr, and Br-BTD(OMe)-Ph, and BTD(OMe)-bis(pBr) (monitored at 480 nm) with excitation at 340 nm. Experimental decay curves are fitted with a double- or triple-exponential function.

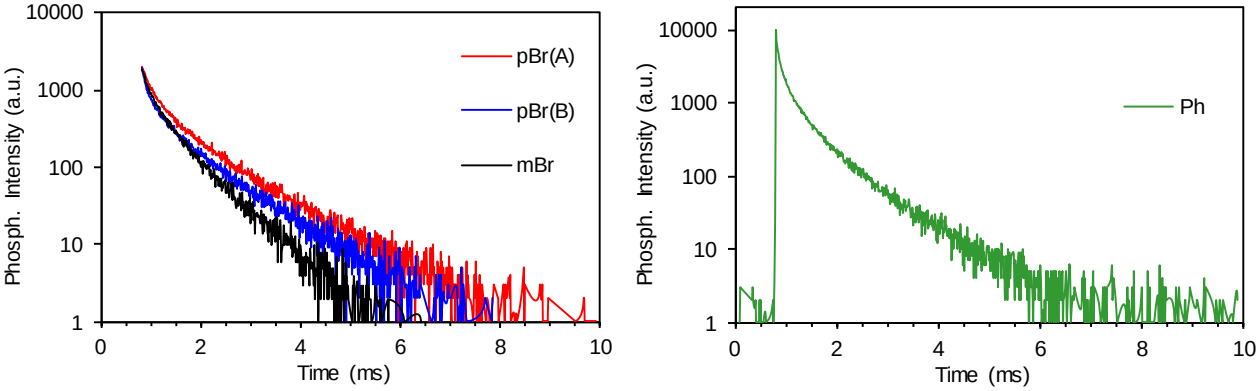

Fig. S10 Phosphorescence decay curves of Br-BTD(OMe)-pBr(A), Br-BTD(OMe)-pBr(B), Br-BTD(OMe)-mBr, and Br-BTD(OMe)-Ph (monitored at 660 nm) with excitation at 340 nm. Experimental decay curves are fitted with a triple-exponential function.

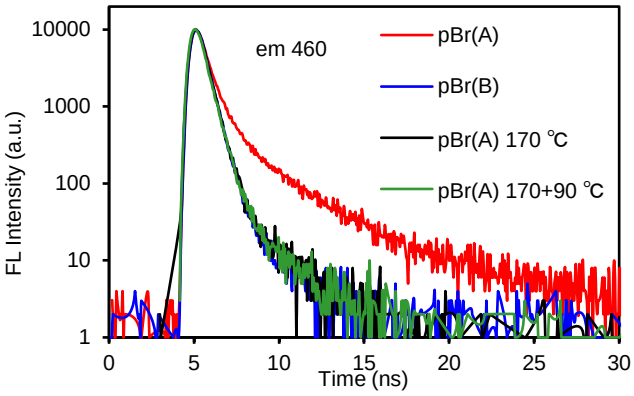

Fig. S11 Fluorescence decay curves of Br-BTD(OMe)-pBr(A) before and after heating at 170 °C and 170+90 °C together with Br-BTD(OMe)-pBr(B) (monitored at 460 nm) with excitation at 340 nm. Experimental decay curves are fitted with a double-exponential function.

Table S4 Fluorescence and phosphorescence lifetime data of benzothiadiazole-based dyes in the crystalline solid state,

Comp.	Fluorescence [a]				Phosphorescence [a]			
	Φ_F (%) [b]	em (nm)	τ_F (ns) (f_i (%)) [c]	$<\tau_F>$ (ns) [d]	Φ_P (%) [b]	em (nm)	τ_P (μs) (f_i (%)) [c]	$<\tau_P>$ (μs) [d]
Br-BTD(OMe)-pBr(A)	0.6	460	0.04 (78) 2.72 (22)	2.60	4.2	660	9.2 (3) 234 (30) 1,046 (67)	971
170 °C	1.0	460	0.03 (89) 1.82 (11)	1.62	~0	660	0.48 (14) 21.5 (34) 64.5 (52)	57
170+90 °C	0.6	460	0.08 (92) 1.93 (8)	1.30	3.5	660	5.8 (3) 177 (36) 813 (61)	740
Br-BTD(OMe)-pBr(B)	1.0	460	0.04 (93) 1.52 (7)	1.17	2.2	660	5.6 (3) 152 (24) 890 (73)	850
Br-BTD(OMe)-mBr	0.6	460	0.02 (87) 2.59 (13)	2.49	1.7	660	3.6 (2) 147 (24) 635 (74)	601
Br-BTD(OMe)-Ph	1.2	460	0.04 (92) 1.54 (8)	1.19	1.2	660	4.9 (6) 137 (39) 720 (55)	649
BTD(OMe)-bis(pBr)	27.6	480	0.14 (3) 1.95 (29) 4.20 (69)	3.83	–	–	–	–

[a] excited at 340 nm, [b] absolute fluorescence and phosphorescence quantum yields determined by an integrating sphere system, [c] the value in parentheses is the fractional contribution of component i to the total steady-state intensity, which was calculated by $f_i = (A_i\tau_{Fi}/\Sigma A_i\tau_{Fi})\times 100$, [d] The intensity-averaged decay lifetime ($<\tau>$) was calculated as follows: $<\tau> = \Sigma(A_n\tau_n^2)/\Sigma(A_n\tau_n)$, in which A_n is the coefficient of each exponential term.

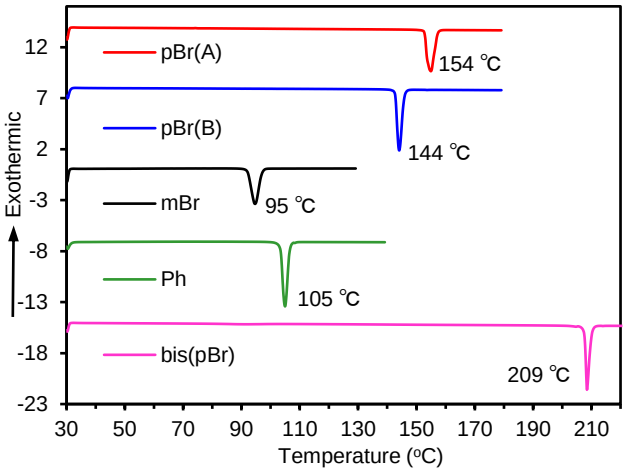

Fig. S12 DSC traces of Br-BTD(OMe)-pBr(A), Br-BTD(OMe)-pBr(B), Br-BTD(OMe)-mBr, Br-BTD(OMe)-Ph, and BTD(OMe)-bis(pBr) in the crystalline solid state.

Table S5 Thermal analysis data obtained from DSC traces.

comp.	state	T_m (°C)	ΔH (kJ mol^{-1})
Br-BTD(OMe)-pBr(A)	as-prepared	154.0	–31.0
	heated/170 °C	77.0	18.0
		143.1	–13.5
		153.5	–14.9
	heated/170+90 °C	153.5	–30.7
Br-BTD(OMe)-pBr(B)	as-prepared	144.1	–30.1
Br-BTD(OMe)-mBr	as-prepared	94.7	–27.2
Br-BTD(OMe)-Ph	as-prepared	105.0	–27.5
BTD(OMe)-bis(pBr)	as-prepared	208.5	–30.0

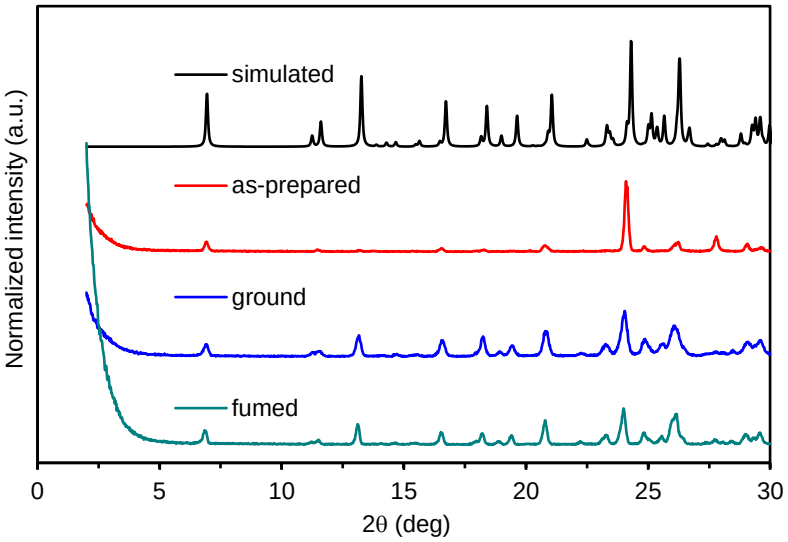

Fig. S13 X-ray diffraction patterns of Br-BTD(OMe)-pBr(A) in the crystalline solid state for the as-prepared, ground, and fumed (dichloromethane-vapor) samples.

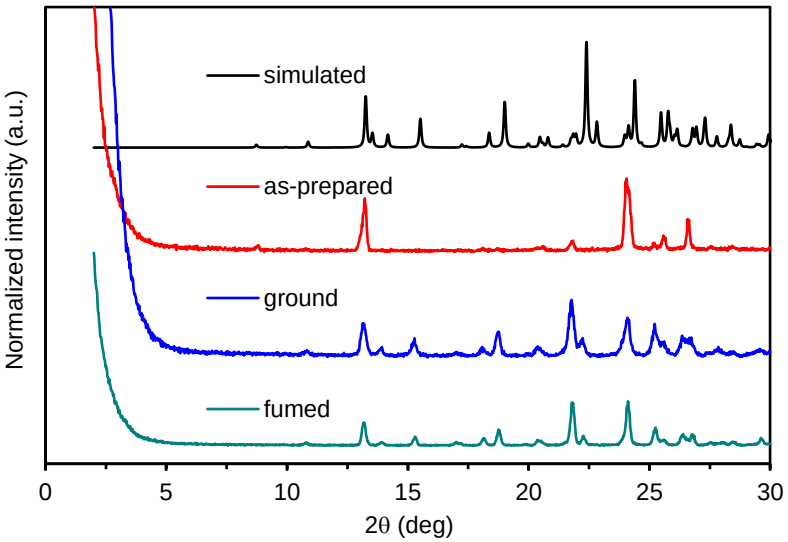

Fig. S14 X-ray diffraction patterns of Br-BTD(OMe)-pBr(B) in the crystalline solid state for the as-prepared, ground, and fumed (dichloromethane-vapor) samples.

Computer simulation analysis.

All quantum chemical calculations based on the time-dependent density functional theory (TD-DFT) were performed using the ADF2023 program package.[1] The structures were calculated as a dimer based on single crystal X-ray structures (Fig. S15). The ground-state (S_0) geometries were initially optimized using the B3LYP functional with the DZP basis set in the gas phase. The vertical excitation calculations were carried out using the optimized S_0 geometries, and the geometry optimizations in the excited S_1 and T_1 states were performed using TD-DFT at the same level of theory. For the $S_0 \rightarrow S_m$ (m = 1−4) and $S_0 \rightarrow T_n$ (n = 1−4) transitions, the natural transition orbitals (NTOs) with their excitation energies were simulated using the optimized S_1 and T_1 geometries, respectively. Using the T_1 geometries, the spin−orbit coupling matrix elements, $\langle S_m|\hat{H}_{\mathrm{SOC}}|T_n\rangle$, were calculated using a scalar relativistic TD-DFT with the two-component zeroth-order relativistic approximation (ZORA)[2] at the same level of theory. The contributions of the three degenerate triplet states ($T_{n,x}$, $T_{n,y}$, and $T_{n,z}$) were taken into account by calculating the root sum square of the real and imaginary parts (Re and Im, respectively) of the matrix elements, as expressed by the following equation:[3]

$$\langle S_m|\hat{H}_{\mathrm{SOC}}|T_n\rangle = \{\sum_{a=x,y,z}(\mathrm{Re}^2\langle S_m|\hat{H}_{\mathrm{SOC}}|T_{n,a}\rangle + \mathrm{Im}^2\langle S_m|\hat{H}_{\mathrm{SOC}}|T_{n,a}\rangle)\}^{1/2}$$

1 ADF2023, SCM, Theoretical Chemistry, Vrije Universiteit, Amsterdam, The Netherlands, http://www.scm.com/.

2 F. Wang and T. Ziegler, *J. Chem. Phys.*, 2005, **123**, 154102.

3 E. Y.-T. Li, T.-Y. Jiang, Y. Chi and P.-T. Chou, *Phys. Chem. Chem. Phys*., 2014, **16**, 26184–26192.

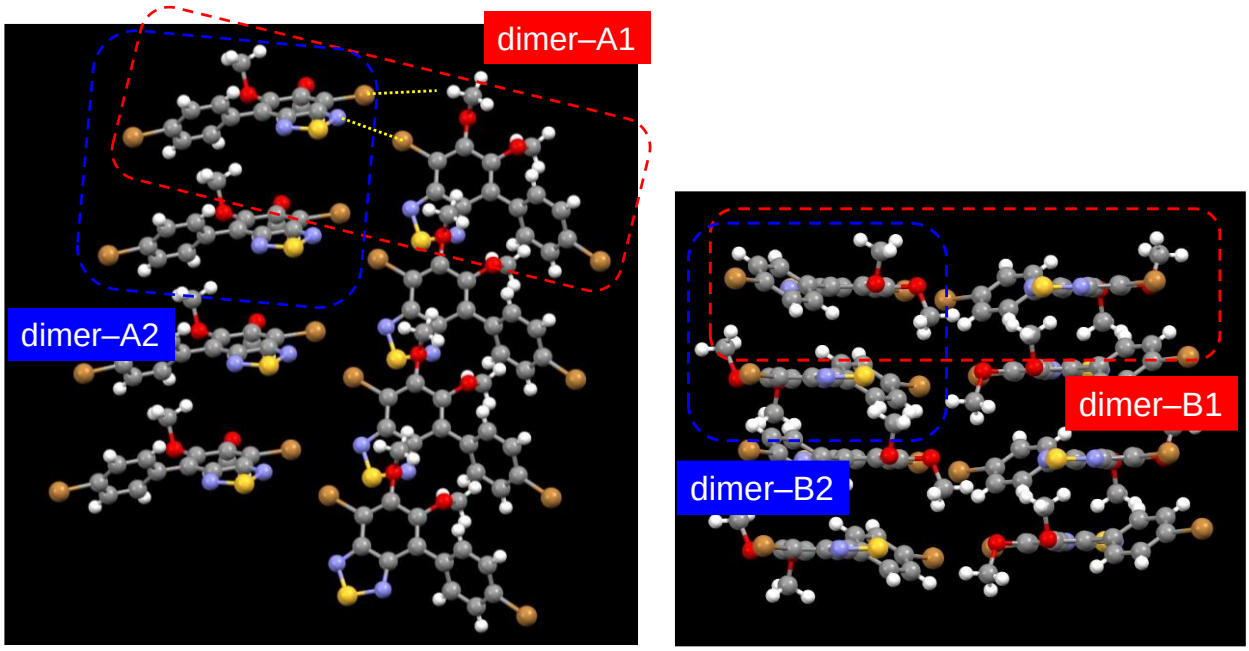

Fig. S15 Structures of dimer-A1 and dimer-A2 in Br-BTD(OMe)-pBr(A), and dimer-B1 and dimer-B2 in Br-BTD(OMe)-pBr(B), which are taken from the crystal packing structure shown in Fig. 4a and 4b. These structures were used in the theoretical calculation.

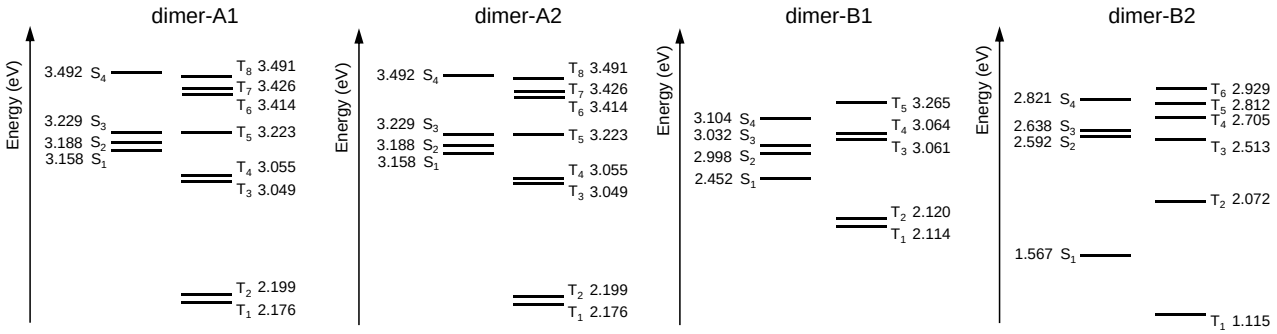

Fig. S16 Theoretical calculated energy diagram for dimer-A1 and dimer-A2 in Br-BTD(OMe)-pBr(A), and dimer-B1 and dimer-B2 in Br-BTD(OMe)-pBr(B).

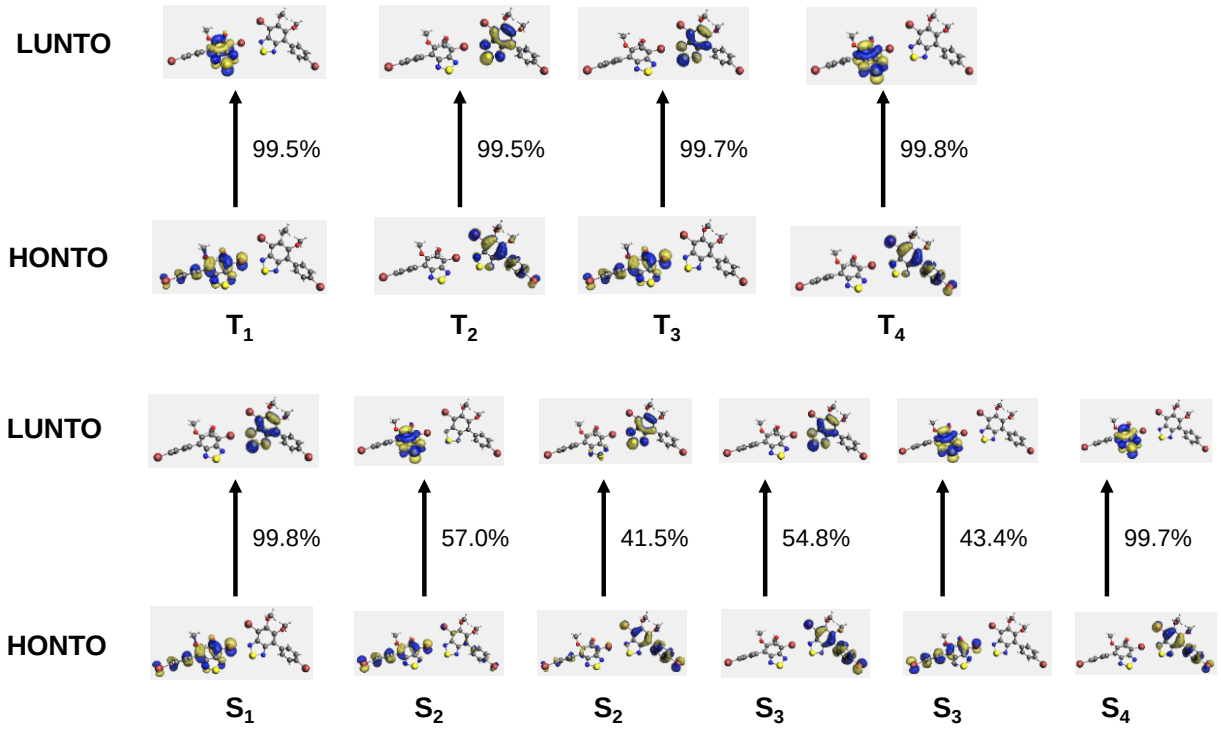

Fig. S17 Theoretical calculated natural transition orbitals (HONTOs and LUNTOs) for dimer-A1 in Br-BTD(OMe)-pBr(A).

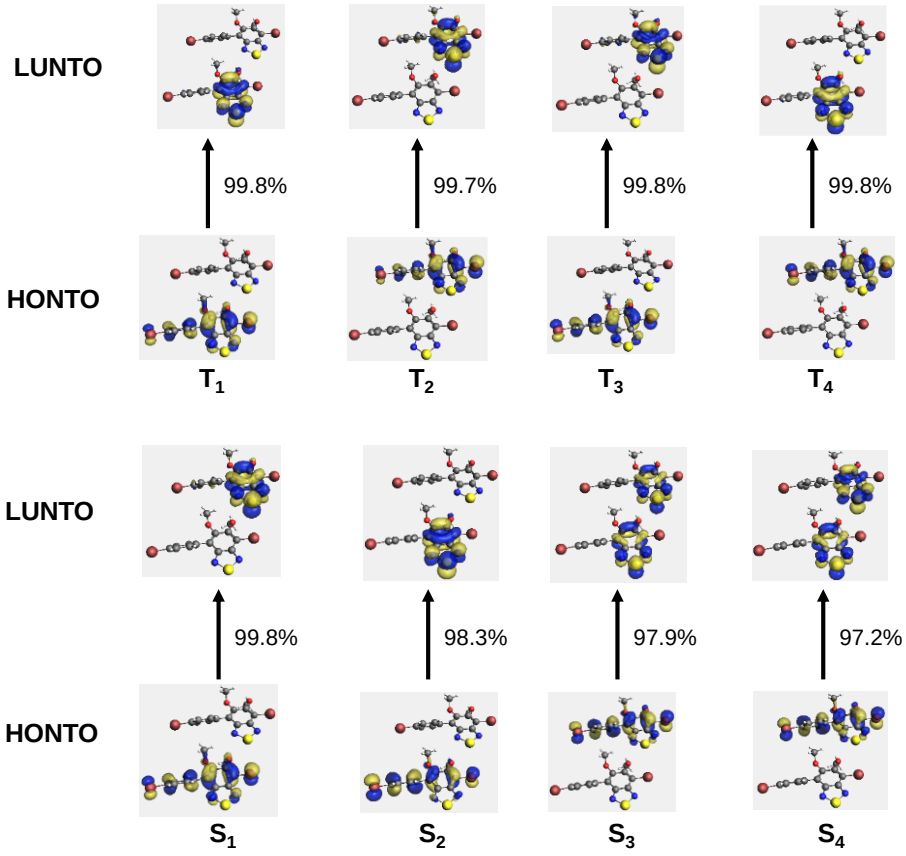

Fig. S18 Theoretical calculated natural transition orbitals (HONTOs and LUNTOs) for dimer-A2 in Br-BTD(OMe)-pBr(A).

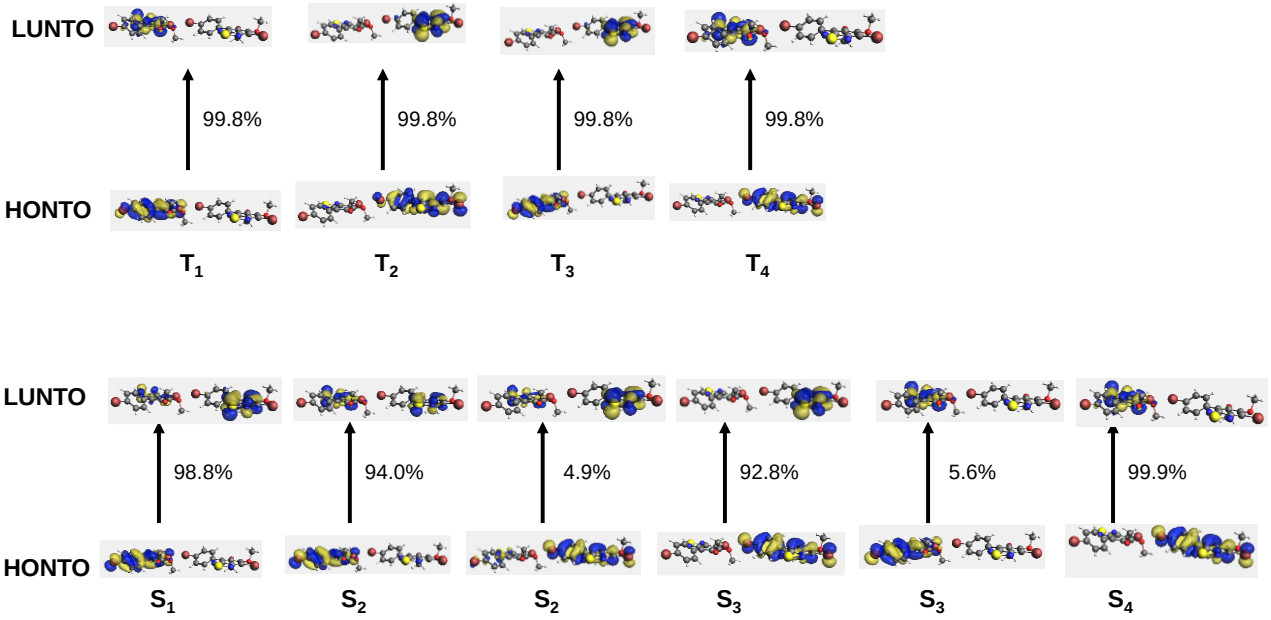

Fig. S19 Theoretical calculated natural transition orbitals (HONTOs and LUNTOs) for dimer-B1 in Br-BTD(OMe)-pBr(B).

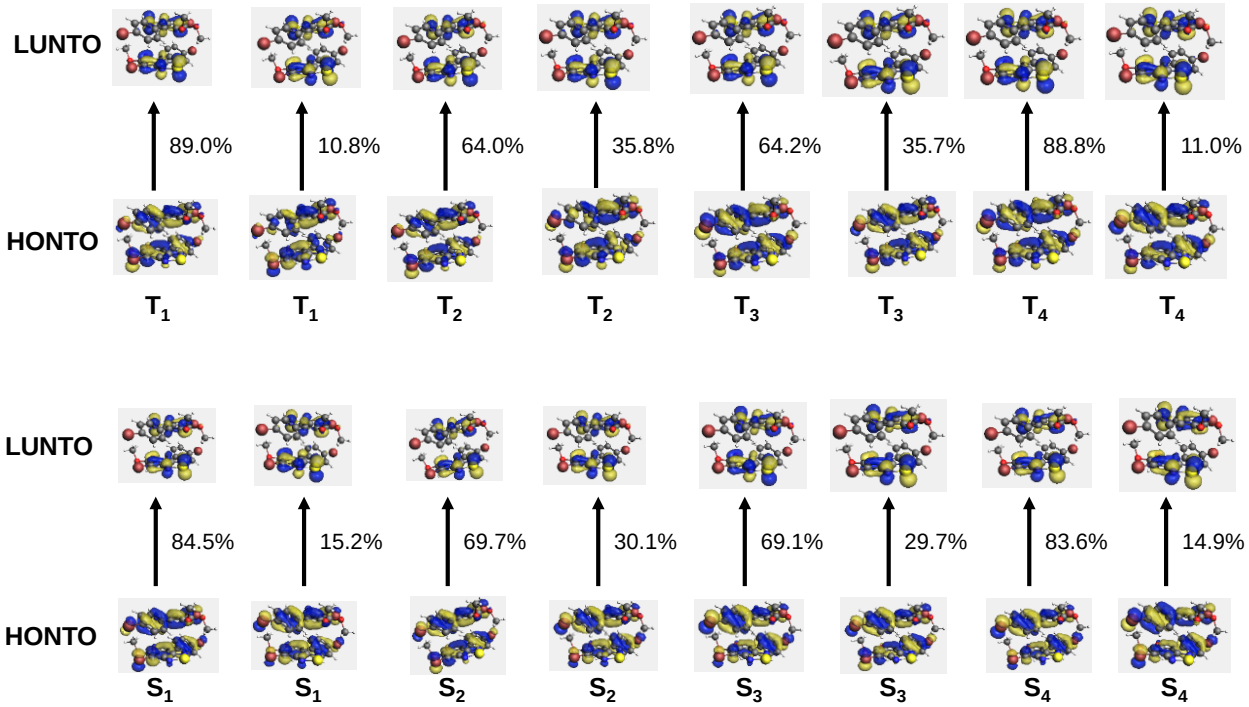

Fig. S20 Theoretical calculated natural transition orbitals (HONTOs and LUNTOs) for dimer-B2 in Br-BTD(OMe)-pBr(B).

Single crystal X-ray diffraction analysis.

The single crystals for the X-ray diffraction analysis were obtained by the slow diffusion of hexane into the dichloromethane solution in Br-BTD(OMe)-pBr(A) (pale yellow prisms), by the slow diffusion of hexane into the chloroform solution in Br-BTD(OMe)-pBr(B) (pale yellow plates), and by the slow diffusion of hexane into the dichloromethane solution in Br-BTD(OMe)-mBr (pale yellow needles).

All measurements were made on a Rigaku XtaLAB Synergy R/DW diffractometer coupled to a Rigaku AFC HyPix-6000 detector with Cu Kα radiation (λ = 1.54184 Å) or Mo Kα radiation (λ = 0.71073 Å). Using Olex2,[1] the structure was solved with the Olex2.solve[2] structure solution program using Charge Flipping and refined with the Olex2.refine[2] refinement package using Gauss-Newton minimization. The non-hydrogen atoms were refined anisotropically. Hydrogen atoms were refined using the riding model. Simulated powder patterns were generated with Mercury 4.2 from the structures determined by single crystal diffraction analyses.[3]

1 O. V. Dolomanov, L. J. Bourhis, R. J. Gildea, J. A. K. Howard and H. Puschmann, OLEX2: A complete structure solution, refinement and analysis program. *J. Appl. Cryst.*, 2009, **42**, 339–341.

2 L. J. Bourhis, O. V. Dolomanov, R. J. Gildea, J. A. K. Howard and H. Puschmann, *Acta Cryst*., 2015, **A71**, 59–75.

3 https://www.ccdc.cam.ac.uk/support-and-resources/Downloads/

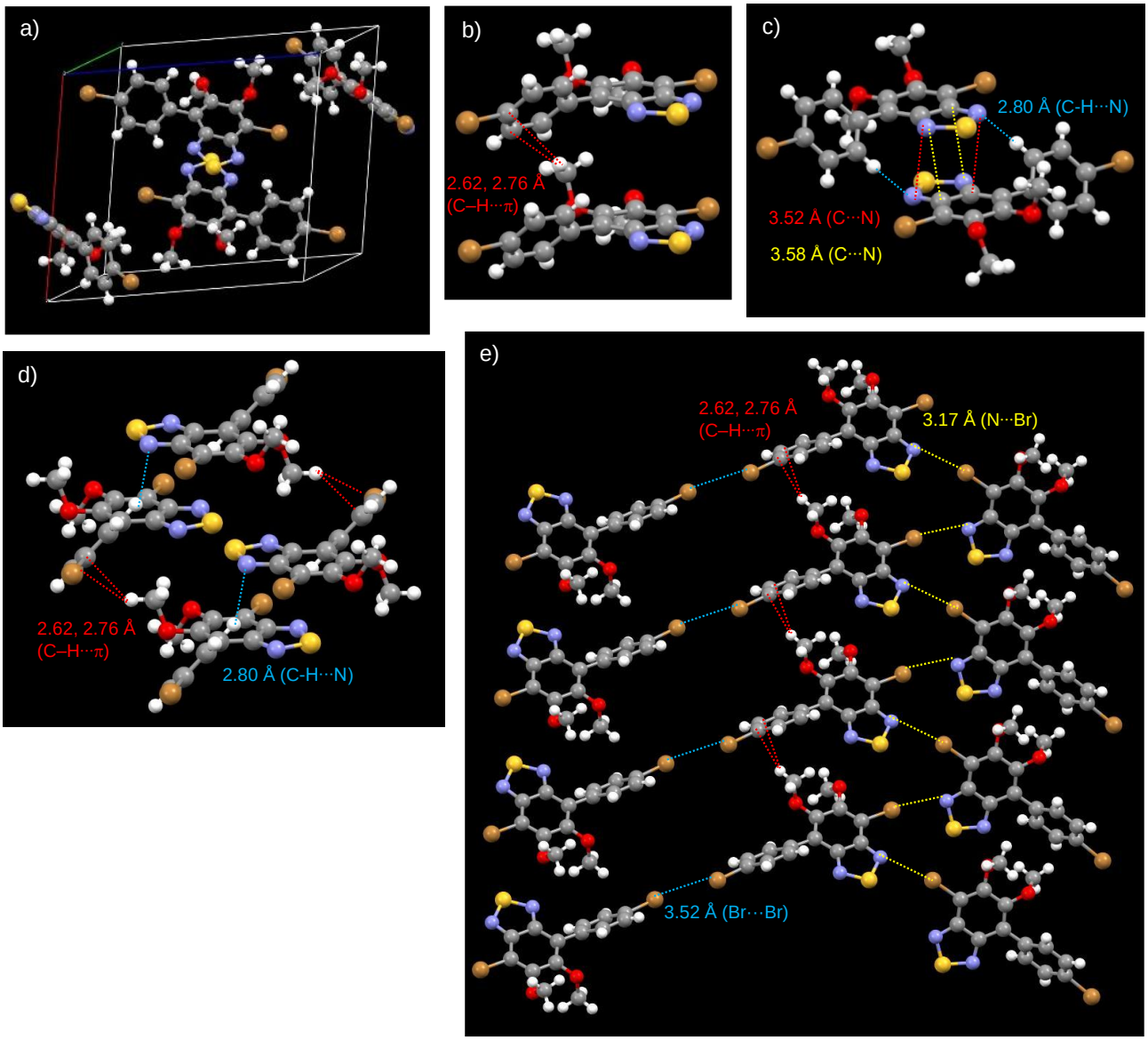

Fig. S21 Single crystal X-ray structure of Br-BTD(OMe)-pBr(A): (a) unit cell packing, (b) parallel dimeric structures in the one-dimensional columnar structure (shown in Fig. 4a in the manuscript), (c) anti-parallel dimeric structure, (d) aggregate structure of two-type dimeric structures (shown in Fig. S21b and S21c), (e) the inter-columnar structure stabilized by network of N···Br interactions and by single Br···Br interactions (this columnar structure is composed of one-dimensional aggregation of the parallel dimers (shown in Fig. S21b).

Due to the intermolecular halogen interactions on the benzothiadiazole moiety and the large number of intermolecular interactions, the inter-system crossing could be accelerated, resulting in the relatively moderate phosphorescence.

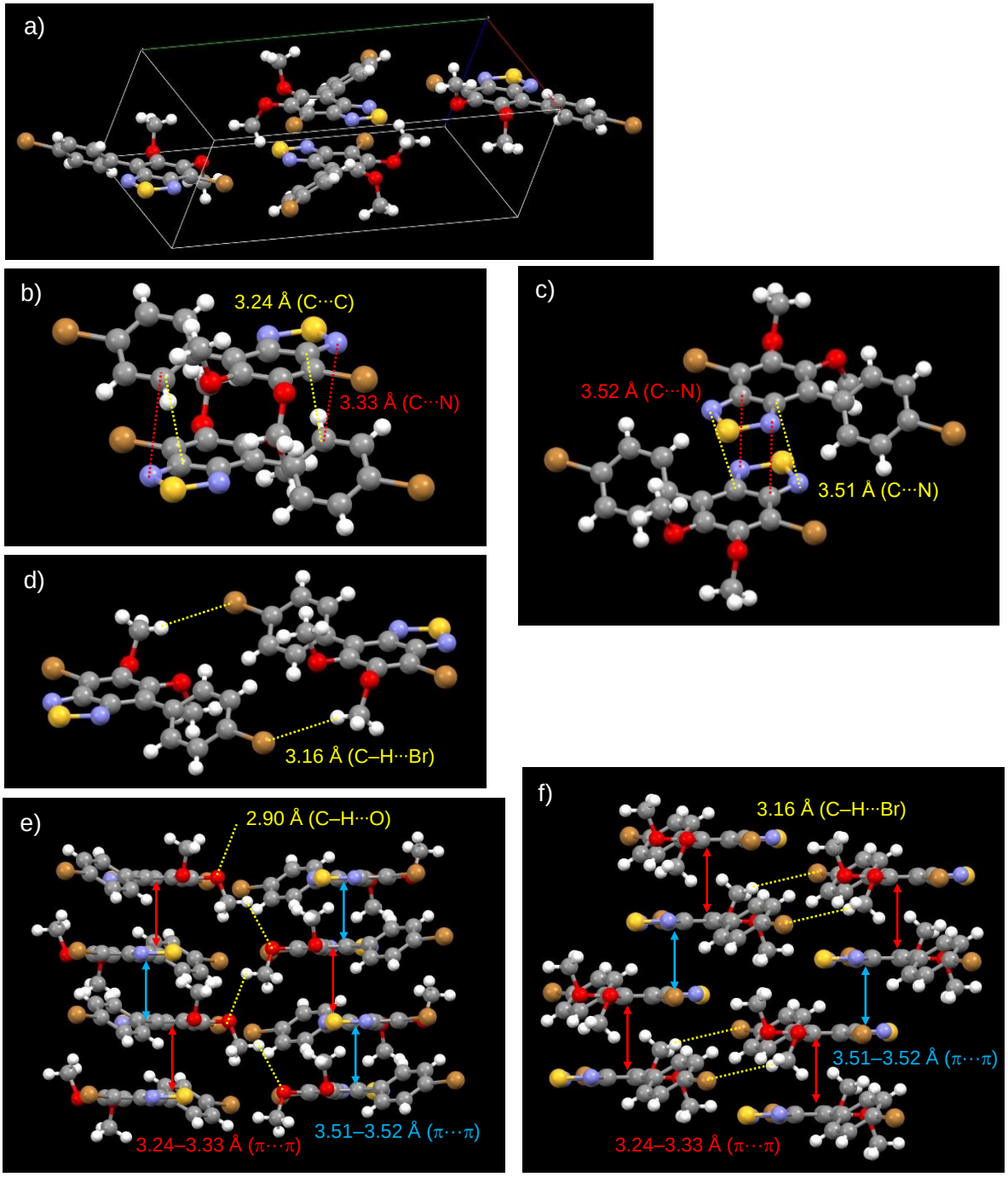

Fig. S22 Single crystal X-ray structure of Br-BTD(OMe)-pBr(B): (a) unit cell packing, (b) and (c) dimeric structures in the one-dimensional columnar structure (shown in Fig. 4b in the manuscript): (b) in the first and second floors and (c) in the second and third floors in the left column of Fig. 4b, (d) dimeric structure connected by two-point C–H···Br interactions, (e) the inter-columnar structure stabilized by network of C–H···O interactions (same data of Fig. 4b in the manuscript), and (f) the inter-columnar structure stabilized by C–H···Br interactions (shown in Fig. S22d)..

Due to the lacking intermolecular halogen interactions on the benzothiadiazole moiety and the small number of intermolecular interactions, the inter-system crossing could not be accelerated, leading to the weak phosphorescence.

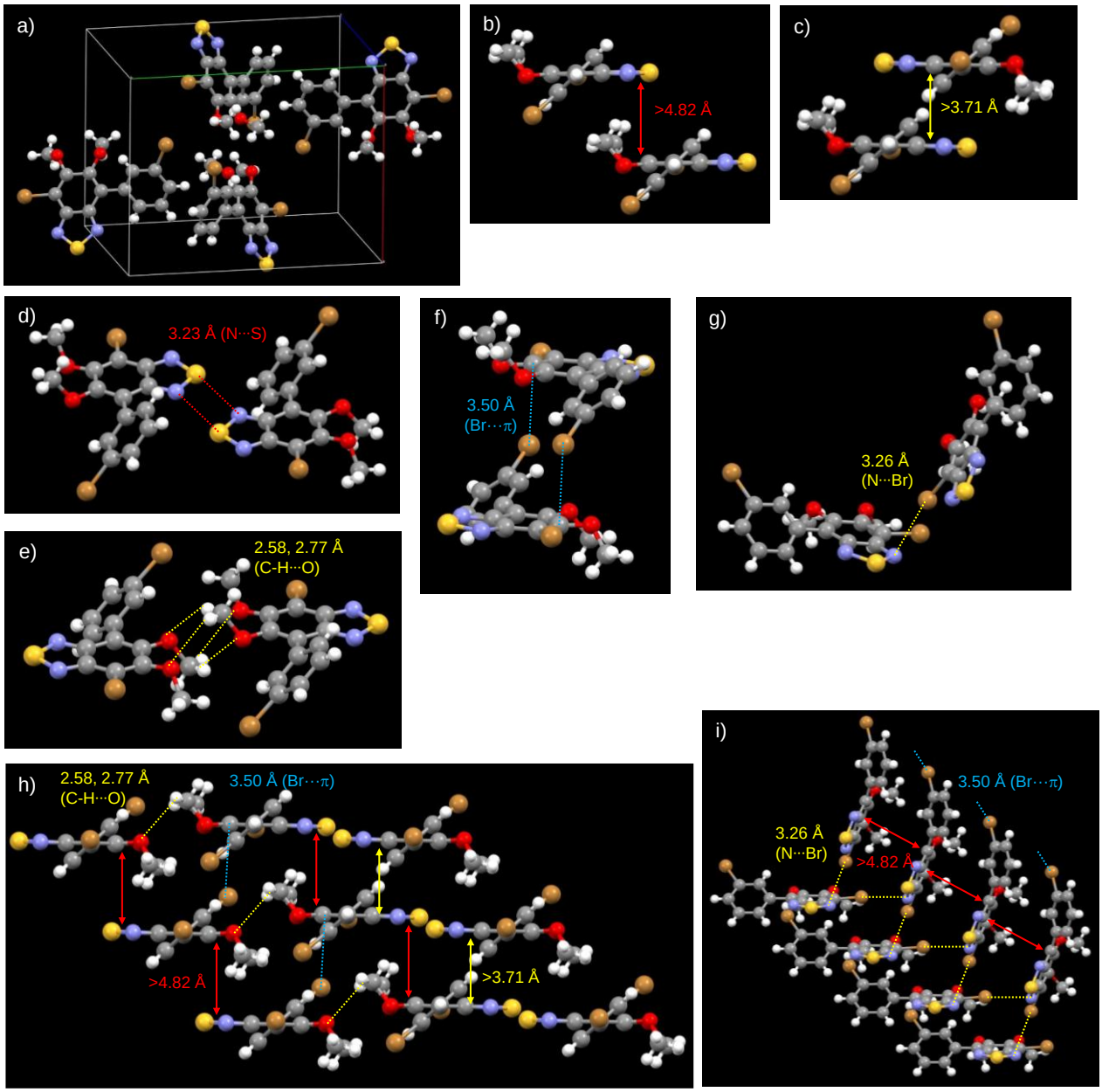

Fig. S23 Single crystal X-ray structure of Br-BTD(OMe)-mBr: (a) unit cell packing, (b) non-stacked parallel dimer, (c) non-stacked anti-parallel dimer, (d) head-to-head dimer with N···S interactions, (e) tail-to-tail dimer with C–H···O interactions, (f) non-stacked anti-parallel dimer with two-point Br···π interactions, (g) the twisted dimeric structure with N···Br interactions (a part structure of Fig. 4c in the manuscript), (h) the inter-columnar structure between the ladder type one-dimensional aggregates through N···S, C–H···O, and Br···π interactions (shown in Fig. S23d, S23e, and S23f): this ladder type aggregate is composed of the non-stacked parallel dimers (shown in Fig. S23b and 23c), (i) the twisted packing structure between the ladder type one-dimensional aggregates through N···Br interactions (shown in Fig. 4c in the manuscript).

Due to the lack of π-stacking interactions and the small number of intermolecular interactions, the inter-system crossing could not be accelerated, nevertheless the presence of the intermolecular halogen interactions on the benzothiadiazole moiety.

Table S6 Selected data for the single crystals of Br-BTD(OMe)-pBr(A), Br-BTD(OMe)-pBr(B), and Br-BTD(OMe)-mBr dyes.

data		Br-BTD(OMe)-pBr(A)	Br-BTD(OMe)-pBr(B)	Br-BTD(OMe)-mBr
Monomer:				
bond length (Å)	C–Br	1.881, 1.906 (on benzene)	1.876, 1.895 (on benzene)	1.884, 1.904 (on benzene)
	C–O	1.363, 1.372 (benzene side)	1.361, 1.373 (benzene side)	1.356, 1.364 (benzene side)
dihedral angle (°)	BTD–benzene	51.15	37.43	43.32
orientation	OMe groups	anti-parallel	anti-parallel	parallel
Stacked dimer:				
intermolecular interactions (Å) (torsion angel (°))	BTD···BTD (π···π)	3.518, 3.579	3.242, 3.329, 3.514, 3.523	–
	Ph···OMe (C–H···π)	2.619 (133.56), 2.763 (151.39)	–	–
	others	2.802 (143.02) (C–H···N)	–	–
Packing:				
intermolecular interactions (Å) (torsion angel (°))	Br interactions	3.170 (169.51) (N···Br), 3.524 (153.23) (Br···Br),	3.161 (160.97°) (C–H···Br),	3.264 (168.25) (N···Br), 3.500 (125.03) (C···Br)
	OMe···OMe (C–H···O)	–	2.903 (115.11)	2.578 (136.50), 2.767 (110.62)
	others	–	–	3.234 (N···S)
Number of intermolecular interactions		19	12	10

Table S7 Crystallographic data for Br-BTD(OMe)-pBr(A), Br-BTD(OMe)-pBr(B), and Br-BTD(OMe)-mBr dyes.

	Br-BTD(OMe)-pBr(A) dichloromethane/hexane	Br-BTD(OMe)-pBr(B) chloroform/hexane	Br-BTD(OMe)-mBr dichloromethane/hexane
CCDC number	2499602	2499603	2499601
formula	$C_{14}H_{10}Br_2N_2O_2S$	$C_{14}H_{10}Br_2N_2O_2S$	$C_{14}H_{10}Br_2N_2O_2S$
M	430.12	430.12	430.12
T [K]	100	100	100
crystal system	monoclinic	monoclinic	monoclinic
space group	$P2_1/c$ (no. 14)	$P2_1/c$ (no. 14)	$P2_1/c$ (no. 14)
a [Å]	13.1781 (3)	9.2163 (4)	12.0683 (4)
b [Å]	7.36850 (10)	20.2448 (8)	16.5725 (5)
c [Å]	16.2703 (3)	8.2360 (4)	7.4621 (2)
α [°]	90	90	90
β [°]	104.869 (2)	105.566 (5)	105.850 (3)
γ [°]	90	90	90
V [Å^3]	1526.99 (5)	1480.33 (12)	1435.69 (8)
Z	4	4	4
ρ_{calcd} [g cm^{-3}]	1.871	1.930	1.990
μ [mm^{-1}]	8.065	5.621	8.578
	μ (Cu Kα)	μ (Mo Kα)	μ (Cu Kα)
F (000)	840	840	840
crystal size [mm^3]	0.13 × 0.12 × 0.08	0.35 × 0.28 × 0.10	0.40 × 0.04 × 0.02
θ range [°]	3.47–75.6	2.29–27.5	3.81–75.1
index range	–15 16	–11 11	–15 15
	–7 9	–22 26	–20 20
	–20 20	–10 10	–5 8
reflections collected	12,422	13,391	10,776
reflections unique	3,144	3,394	2,777
R_{int}	0.0330	0.0270	0.0405
data [$F^2 > 2\sigma$ (F^2)]	3,003	3,081	2,911
parameters	192	192	192
goodness-of-fit	1.071	1.068	1.074
$R1/wR^2$ [$F^2 > 2\sigma$ (F^2)]	0.0286/0.0780	0.0283/0.0584	0.0307/0.0834
$R1/wR^2$ (all data)	0.0300/0.0792	0.0337/0.0600	0.0319/0.0844
Resd. min/max [eÅ^{-3}]	–0.72/0.56	–0.44/0.45	–0.57/1.01
Max Shift/error in final cycle	0.002	0.001	0.002

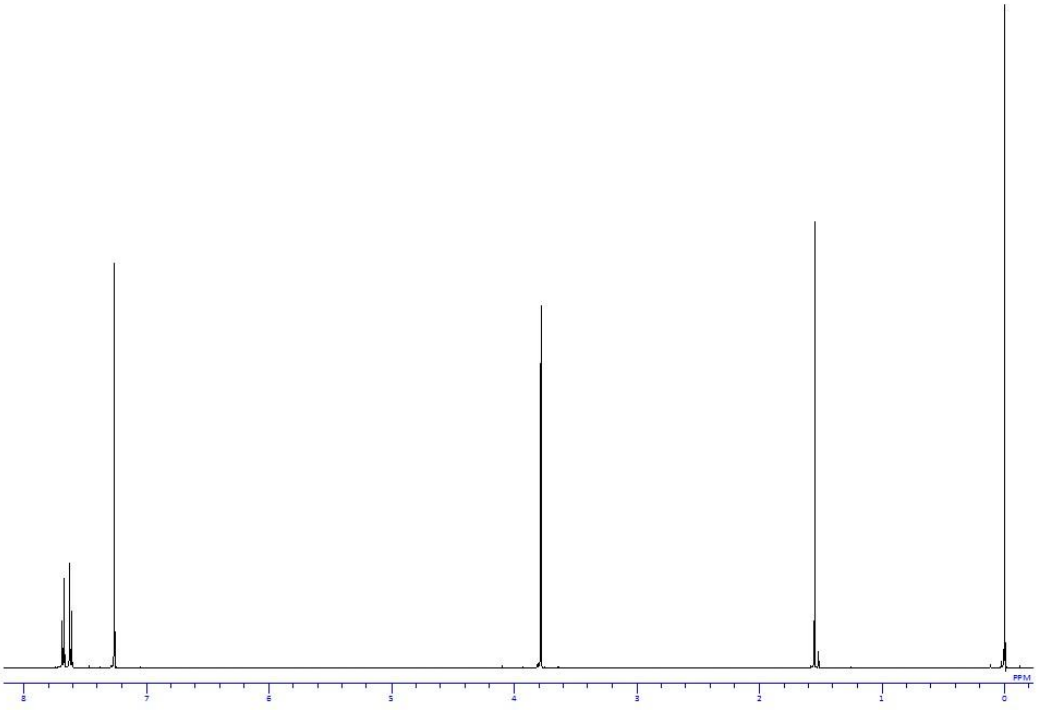

Fig. 24 ^{1}H NMR spectrum of BTD(OMe)-bis(pBr) in $CDCl_3$ at room temperature.

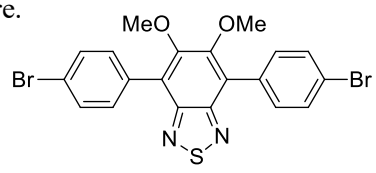

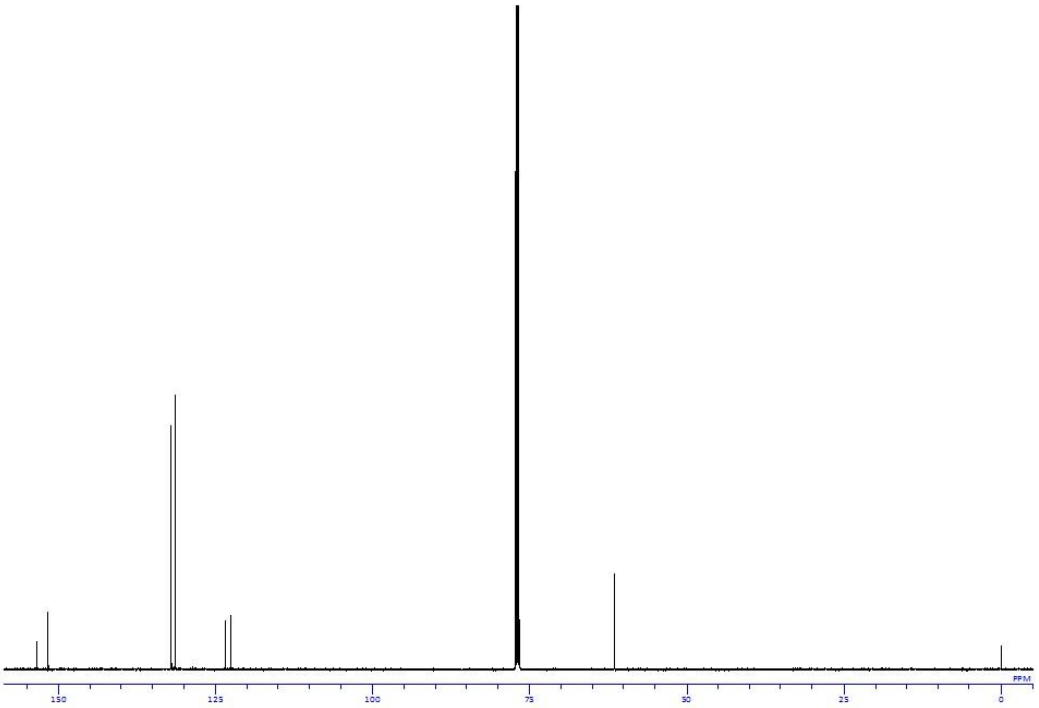

Fig. 25 ^{13}C NMR spectrum of BTD(OMe)-bis(pBr) in $CDCl_3$ at room temperature.

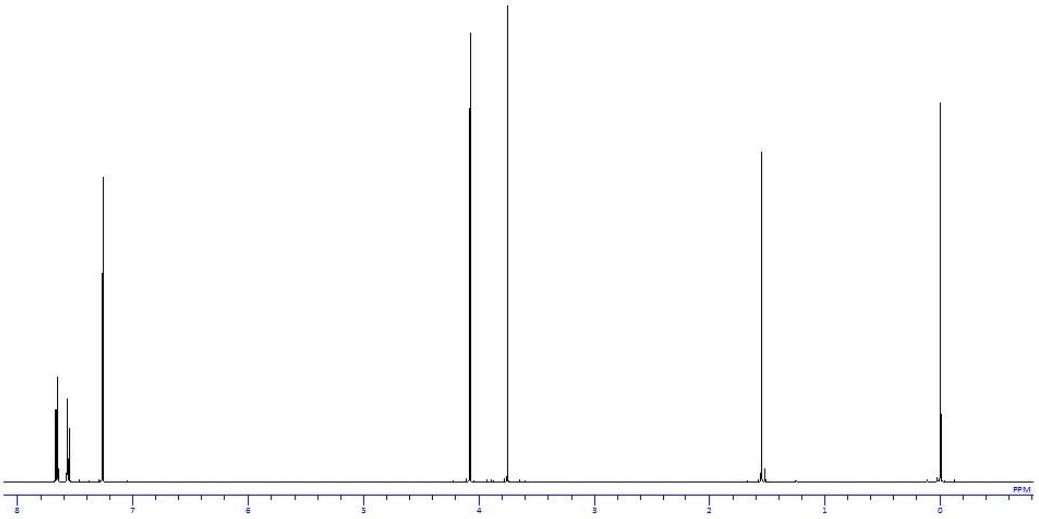

Fig. 26 ^{1}H NMR spectrum of Br-BTD(OMe)-pBr in $CDCl_3$ at room temperature.

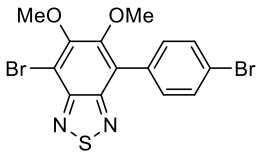

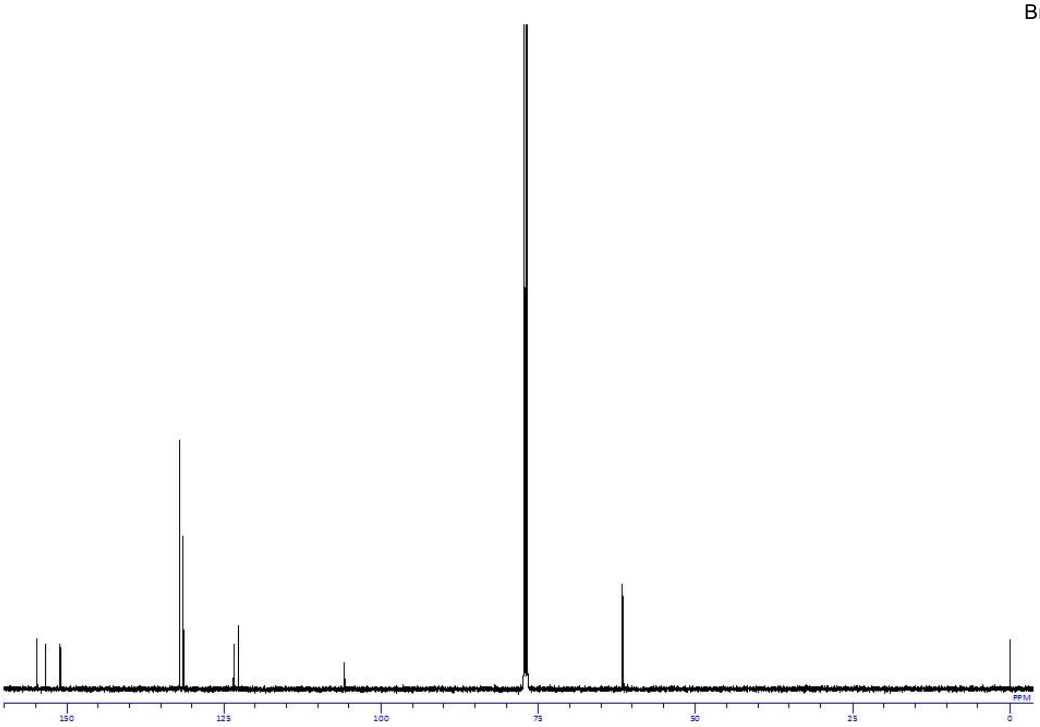

Fig. 27 ^{13}C NMR spectrum of Br-BTD(OMe)-pBr in $CDCl_3$ at room temperature.

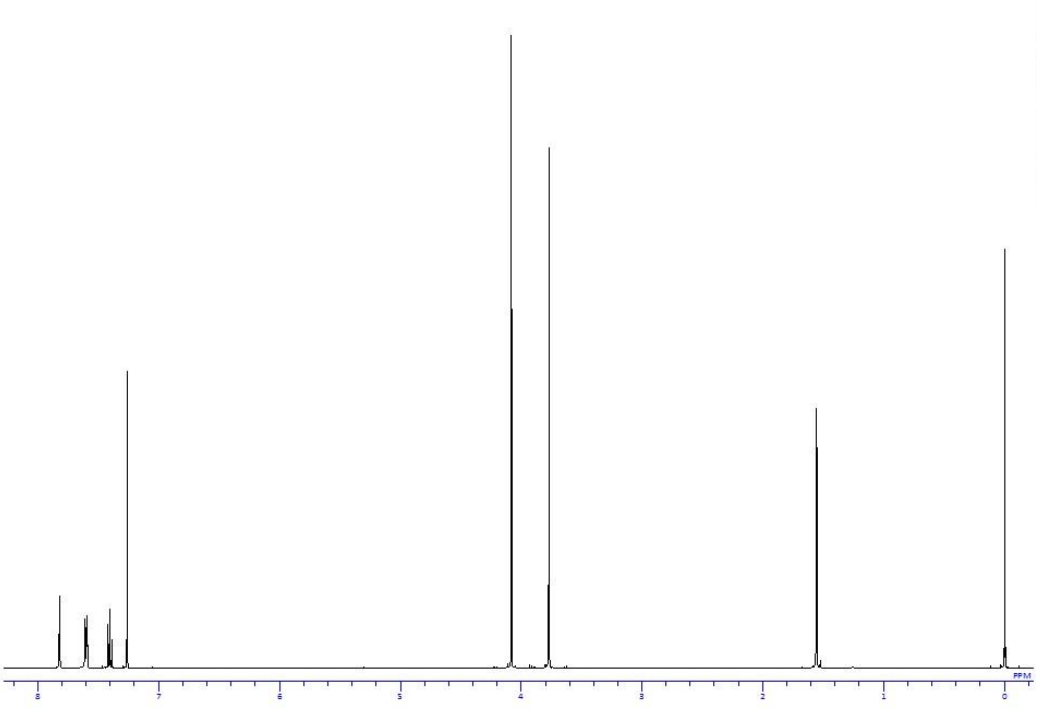

Fig. 28 ^{1}H NMR spectrum of Br-BTD(OMe)-mBr in $CDCl_3$ at room temperature.

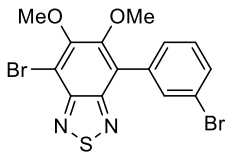

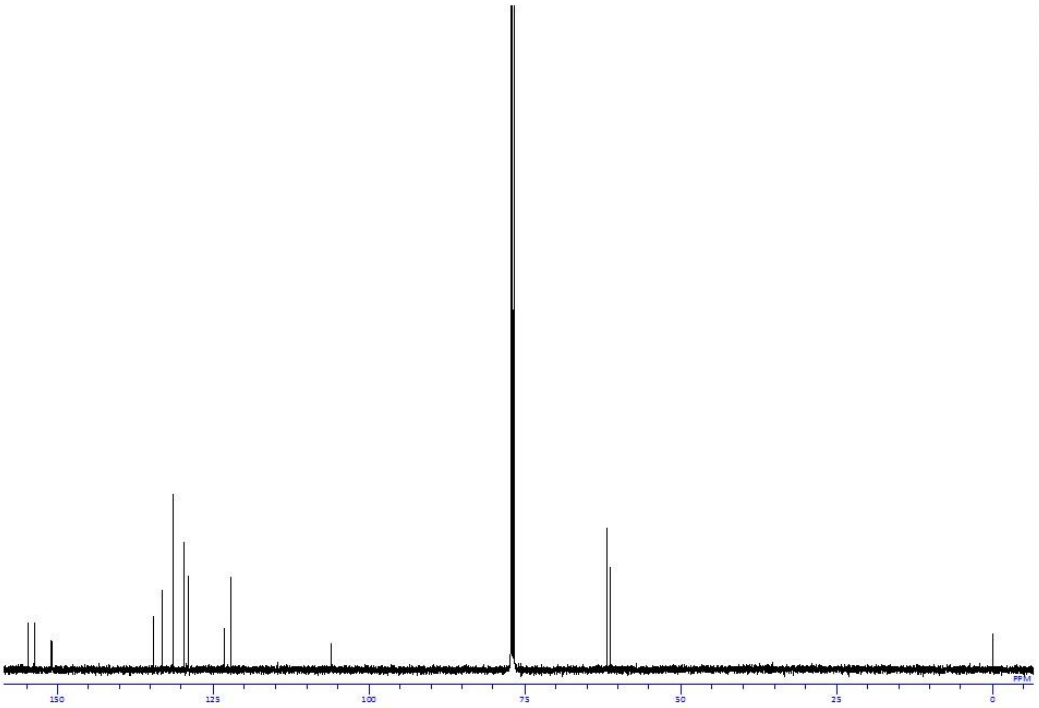

Fig. 29 ^{13}C NMR spectrum of Br-BTD(OMe)-mBr in $CDCl_3$ at room temperature.

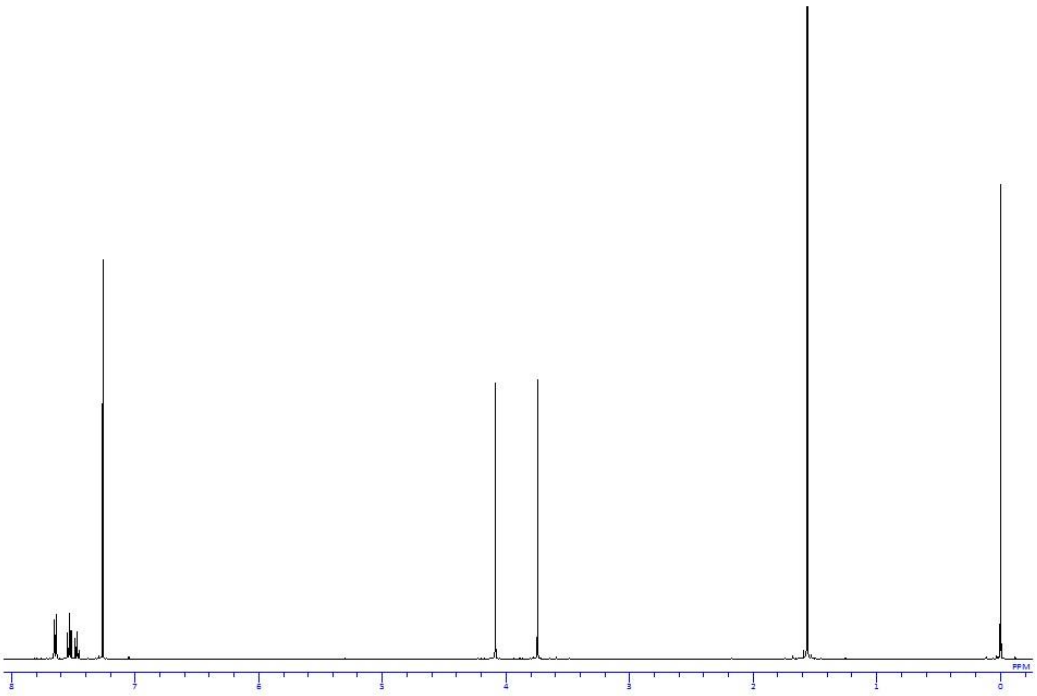

Fig. 30 ^{1}H NMR spectrum of Br-BTD(OMe)-Ph in $CDCl_3$ at room temperature.

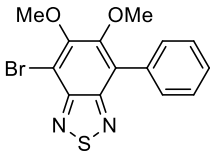

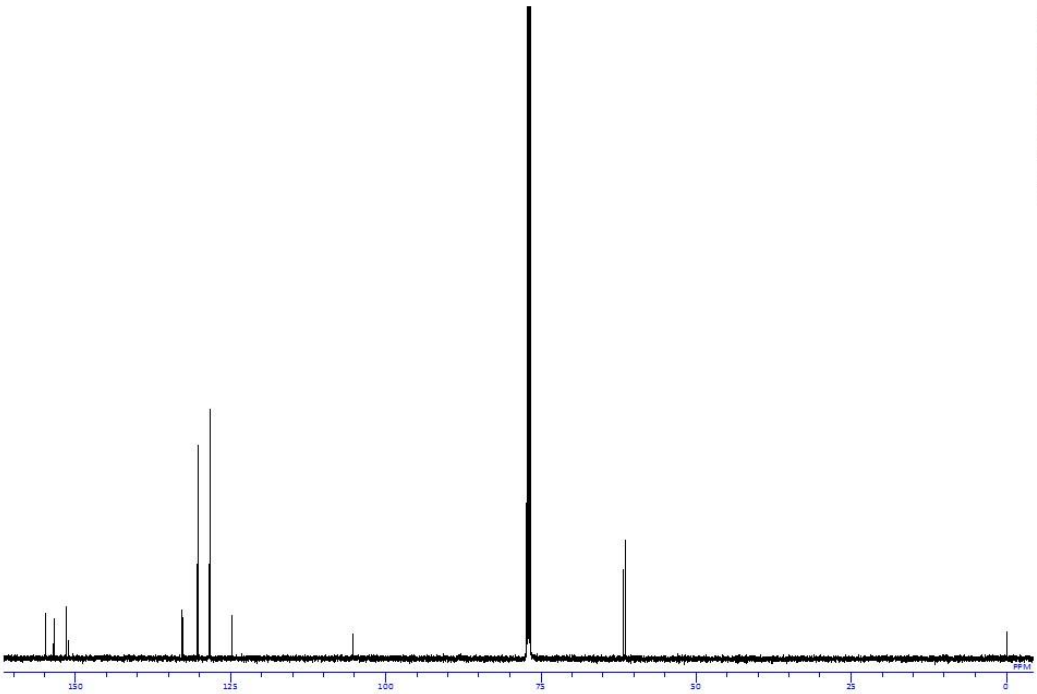

Fig. 31 ^{13}C NMR spectrum of Br-BTD(OMe)-Ph in $CDCl_3$ at room temperature.